Six new species of lizards (*Riama*, Sauria, Gymnophthalmidae) from the high Andes of Ecuador

http://zoobank.org/99F1AB0F-38D9-45E1-9B7B-1C37553FF847

DOI https://doi.org/10.47051/GZNM5526

Alejandro Arteaga,[a,b] Angie Tovar-Ortiz,[c] Jose Vieira,[b,d] Henrik Bringsøe,[e] Amanda Quezada,[a,b] Jeffrey Camper,[f] Kyle Harris.[g]

[a]Khamai Foundation, Arlequín Reserve, Ecoruta Paseo del Quinde km 56, Santa Rosa de Mindo, Ecuador. [b]Tropical Herping S.A., Av. Portugal N35-40 y República del Salvador, Quito, Ecuador. [c]Department of Biological Sciences, Universidad de los Andes, Bogotá, Colombia. [d]ExSitu, Quito, Ecuador. [e]Irisvej 8, 4600 Køge, Denmark. [f]Department of Biology, Francis Marion University, Florence, South Carolina, USA. [g]Department of Biology, Liberty University, Lynchburg, Virginia, USA.

ABSTRACT

We describe six new species of burrowing lizards of the genus *Riama* Gray, 1858 from the high Andes of Ecuador. Their status as new species is confirmed based on their unique combination of molecular, meristic, hemipenial, and color pattern characteristics. The taxonomic revision is based on examination of 188 museum specimens, a phylogeographic analysis of 244 locality records, and 53 individuals of *Riama* sampled for molecular characters. With these additions, the number of *Riama* in Ecuador increases to 18.

INTRODUCTION

The fossorial lizard genus *Riama* Gray, 1858 comprises 21 species native to the high Andes of Colombia and Ecuador. Due to their narrow montane distributions and burrowing habits, they remain among the most elusive and understudied lizards globally. The first comprehensive revision of the group was conducted by Kizirian (1996), who described 16 species (then classified under *Proctoporus* Tschudi, 1845), including 11 of the 12 species currently recognized in Ecuador (Arteaga et al. 2024). Kizirian's work detailed geographic variation, distribution, and morphology, including hemipenial characters.

Subsequent studies by Aguirre-Peñafiel et al. (2014) described a 12th species, *Riama yumborum*, from Ecuador and provided a molecular phylogeny for eight members of the genus. This phylogeny was later completed by Torres-Carvajal et al. (2016) and Sánchez-Pacheco et al. (2018). Despite these efforts, taxonomic uncertainties persist. Several populations identified by Kizirian (1996) as potentially distinct taxa remained unsampled, as did populations of *R. anatoloros*, *R. colomaromani*, *R. stigmatoral*, and *R. unicolor* that exhibit remarkable geographic variation.

In this study, we address these knowledge gaps by integrating molecular and morphological data. We describe six new species of *Riama* endemic to the Ecuadorian Andes, one of which likely extends into neighboring Perú.

MATERIALS AND METHODS

Ethics statement: This study was carried out in accordance with the guidelines for use of live amphibians and reptiles in field research (Beaupre et al. 2004) compiled by the American Society of Ichthyologists and Herpetologists (ASIH), the Herpetologists' League (HL) and the Society for the Study of Amphibians and Reptiles (SSAR). All procedures with animals (see below) were reviewed by the Ministerio del Ambiente, Agua y Transición Ecológica (MAATE) and specifically approved as part of obtaining the following field permits for research and collection: MAE-DNB-CM-2018-0105 and MAATE-DBI-CM-2022-0245.

Voucher material statement: Museum vouchers labeled AAS, CAMPO, JMG, KM, TH, SC, and SCA have been physically housed at the Fundación Herpetológica Gustavo Orcés (FHGO) since 7 April 2025. To date, however, these specimens have not been assigned final accession numbers, which has prevented their formal cataloguing and use as comparative material, including for those specimens serving as name-bearing types. Multiple attempts to obtain clarification regarding this situation—including email correspondence, phone calls, and an in-person meeting on 24 August 2025—did not receive a response. We initially assumed that the delay might have been due to missing documentation (e.g., mobilization guides), and we subsequently provided materials intended to resolve this issue. Nevertheless, communication remained unresolved until 24 August 2025, when we were informed that the specimens would neither receive final accession numbers by the current curator nor be returned to us to be deposited elsewhere, irrespective of documentation.

As a result, the material listed above remains in custody of the FHGO, albeit effectively uncurated, contrary to its intended purpose and to local regulations requiring licensed natural history collections to catalogue specimens in a timely manner. We do not attempt here to assess the causes underlying this situation. We note, however, that the absence of final accession numbers has impeded the publication of this study, as two taxonomic journals suspended review for extended periods and ultimately declined the manuscript on this basis.

We emphasize the importance of assigning final accession numbers to type material and of properly cataloguing and making available alcohol-preserved comparative specimens. We further support the publication of new species descriptions in peer-reviewed journals dedicated to systematic research. Most importantly, timely dissemination of taxonomic findings is essential for both the advancement of systematics and the conservation of the species described herein. We therefore present our results here with the expectation that final accession numbers will be assigned by an appropriate museum authority in the foreseeable future.

Morphological data and analyses: The diagnoses and descriptions, including terminology for cephalic shields in *Riama*, follow Kizirian (1996). We examined fluid-preserved specimens from the herpetology collections of the American Museum of Natural History (AMNH), the Academy of Natural Sciences of Philadelphia (ANSP), and the Fundación Herpetológica Gustavo Orcés (FHGO). The dataset comprised 188 individuals, including 21 specimens of *Andinosaura* and *Riama* (see Supplementary file 1).

Morphometric variables measured are listed in Supplementary file 1. Morphometric analyses were conducted independently for three groups (Groups 1–3) defined *a priori* based on molecular phylogenetic results (see Results) and hypothesized to represent distinct species. To minimize allometric effects, morphometric variables were size-corrected by regressing each variable against SVL and extracting standardized

residuals (Thorpe 1975; Lleonart et al. 2000). A multivariate analysis of variance (MANOVA) was then performed using species as a factor, with SVL and the residuals of FNL, FL, and CL as dependent variables. Variables not showing significant differences were excluded from subsequent analyses.

Morphometric clustering was assessed using k-means clustering on the size-corrected dataset, testing values of K from 3 to 6 (Hartigan and Wong 1979). The optimal number of clusters was evaluated using silhouette widths (Rousseeuw 1987), the Calinski–Harabasz criterion (Caliński and Harabasz 1974), and the elbow method (Thorndike 1953). Morphometric variation was further summarized using principal component analysis (PCA) based on the correlation matrix, retaining components with eigenvalues >1 and applying Varimax rotation (Kaiser 1958). Group assignments were evaluated using individual scores on retained components. All analyses were performed independently for each group.

Scale count data were analyzed using a similar clustering framework but without size correction. Clustering of categorical scale characters was conducted using the k-modes algorithm implemented in the R package *klaR* (Weihs et al. 2005). Variation in scale counts was summarized using multiple correspondence analysis (MCA), which is appropriate for categorical data and allows identification of associations among scale traits (Greenacre 2007). Dimensions were selected based on scree plots and the proportion of variance explained.

All statistical analyses were conducted in R (R Core Team 2023) using the packages *stats*, *cluster*, *factoextra*, *ggplot2*, *klaR*, and *FactoMineR* (Lê et al. 2008; Wickham 2016; Kassambara and Mundt 2020; Maechler et al. 2023). Reproducibility was ensured by setting a fixed random seed (set.seed[123]).

Hemipenial morphology: Hemipenes were prepared from museum specimens using the procedures of Pesantes (1994) and Zaher (1999). Hemipenial terminology is based on Dowling and Savage (1960), Kizirian (1996), Zaher (1999), and Sánchez-Pacheco et al. 2018.

Sampling and laboratory techniques: Genomic DNA was extracted from tissue samples (liver, muscle, or scales) and preserved in 96% ethanol using either a guanidinium isothiocyanate protocol (Peñafiel et al. 2020) or a modified salt-precipitation method based on the Puregene DNA purification kit (Gentra Systems). Primer sequences and PCR conditions for each locus are provided in Appendix I. PCR products were purified using either ExoSAP-IT (Affymetrix, Cleveland, OH) or Exonuclease I and alkaline phosphatase (ExoProStar; GE Healthcare), and subsequently sequenced by Macrogen Inc. (Seoul, South Korea) using Sanger sequencing. All amplicons were sequenced in both forward and reverse directions with the same primers used for amplification. Sequence data were generated for samples indicated with an asterisk in Supplementary file 2. All sequences were deposited in GenBank, and accession numbers are provided in Supplementary file 2.

DNA phylogenetic analyses: A total of 211 DNA sequences were used to infer phylogenetic relationships within *Riama*, including 78 sequences generated in this study and 133 obtained from GenBank (Supplementary file 2). The dataset comprised fragments of four loci: 12S (19 sequences; 333–393 bp), 16S (20; 432–500 bp), CMOS (19; 378–384 bp), and ND4 (20; 447–623 bp). Newly generated sequences were edited and assembled in Geneious Pro™ 2021.1.1 (Drummond et al. 2021) and aligned with published sequences using MAFFT v7 (Katoh and Standley 2013) under default settings.

Gene fragments were concatenated into a single matrix partitioned into eight subsets: one partition for each non-coding gene and three partitions per protein-coding gene corresponding to codon positions. Optimal partitioning schemes and models of nucleotide substitution were selected in PartitionFinder 2.1.1 (Lanfear et al. 2016) using the Bayesian Information Criterion.

Phylogenetic inference was conducted using Bayesian inference (BI) in MrBayes 3.2.0 (Ronquist and Huelsenbeck 2013). Four independent runs were performed to reduce the risk of convergence on local optima. Each run consisted of 6,666,667 generations with four Markov chains and default heating parameters. Trees were sampled every 1,000 generations, and the first 25% were discarded as burn-in. The remaining trees were combined to estimate posterior probabilities for each node in a 50% majority-rule consensus tree.

Convergence and sampling adequacy were assessed in Tracer 1.6 (Rambaut et al. 2022) by examining effective sample sizes (ESS) for all parameters. Additionally, we confirmed that the average standard deviation of split frequencies across runs was ≤0.01.

Distribution maps and ecological niche models: We present range maps for seven species of *Riama* from Ecuador. Occurrence records were compiled from museum vouchers (Supplementary file 1), photographic records (iNaturalist), and published literature, and are summarized in Supplementary file 3. For two species, we present both dot maps and binary environmental niche models (ENMs). ENMs estimate potential distributions based on known occurrences and environmental predictors (Elith and Leathwick 2009). To delimit areas of occupancy and potential distributions, we followed the BAM framework (Soberón and Peterson 2005; Peterson et al. 2011).

Models were constructed using presence localities from Supplementary file 3, 19 bioclimatic variables from WorldClim v1.4 (Hijmans et al. 2005), and Maxent v3.4.1k, which implements a maximum entropy algorithm (Phillips et al. 2006; Elith et al. 2011; Renner and Warton 2013). In an initial exploratory analysis, all 19 climatic variables were included, and variable importance was evaluated using the jackknife test implemented in Maxent (Royle et al. 2012). Highly correlated variables (Pearson's $r \geq 0.8$) were identified using Pearson correlation tests in PAST v3 and excluded from subsequent analyses.

In a second modeling step, ENMs were generated using the reduced set of uncorrelated variables. Models were run with 5,000 iterations, clamping enabled, and extrapolation disabled; all other parameters were retained at default settings. Habitat suitability was estimated using the logistic output format, yielding continuous suitability values ranging from 0 to 1. Binary ENMs were produced by applying a minimum training presence threshold to distinguish suitable from unsuitable areas. For these analyses, the convergence threshold was set to 10^{-5}, the maximum number of iterations to 500, and the regularization parameter to "auto."

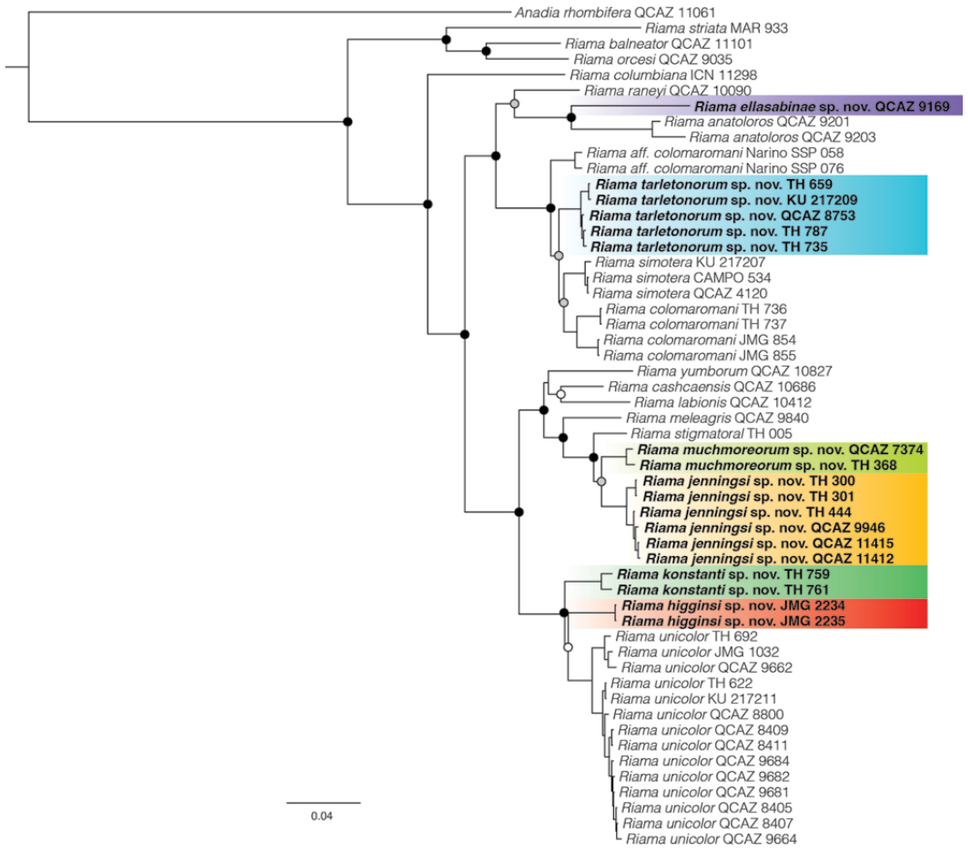

Figure 1: Phylogenetic relationships within *Riama* inferred using a Bayesian inference and derived from analysis of DNA gene fragments 12S, 16S, ND4, and CMOS. Support values on intra-specific branches are not shown for clarity. Voucher numbers for sequences are indicated for each terminal. Black dots indicate clades with posterior probability values from 95–100%. Gray dots indicate values from 70–94%. White dots indicate values from 50–69% (values <50% not shown). Colored clades correspond to the species' distribution presented in Fig. 2.

Rationale for species delimitation: We define species as independent evolutionary lineages following the General Lineage Concept (de Queiroz 2007). To identify species boundaries, we employ an "integration by congruence" approach (Padial et al. 2010), requiring support from at least two independent lines of evidence. We initiated the delimitation process by identifying mitochondrial clades with > 3% sequence divergence (mean p-distance) in a 500-bp fragment of the 16S gene. This threshold reflects species-level differences observed in other *Riama* species pairs, including *R. labionis–R. yumborum* (Aguirre-Peñafiel et al. 2014). We then tested the validity of these lineages by assessing their diagnostic distinctness across the following four phenotypic datasets: (1) lepidosis, (2) hemipenial morphology, (3) coloration, and (4) body size. Finally, we evaluated

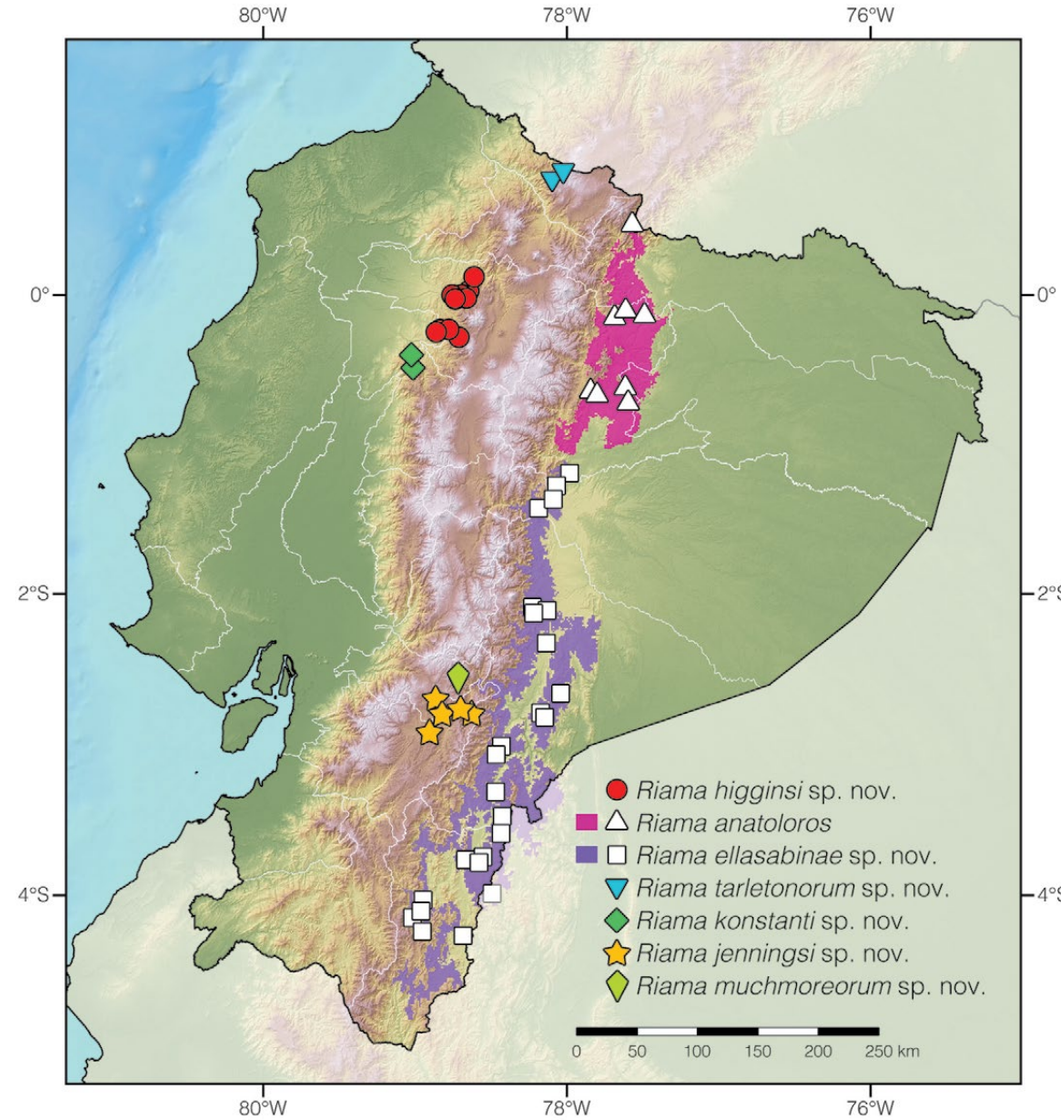

Figure 2: Distribution of seven species of *Riama* in Ecuador, including the six new species described in this work. Each colored area is a geographic representation of the suitable environmental conditions for one of the clades recovered in the phylogeny of Fig. 1.

geographical and ecological congruence using environmental niche models. Consequently, we recognize taxa as species only if they are monophyletic, exceed the 3% genetic threshold, and are morphologically and biogeographically diagnosable.

RESULTS

Molecular phylogeny: We consider strong support for clades as Bayesian posterior probabilities (BPP) > 95% (Felsenstein 2004). Our topology (Fig. 1) resembles the

relationships proposed by Torres-Carvajal et al. (2016) and Sánchez-Pacheco et al. (2018). Below, we detail minor topological differences and outline the phylogenetic placement of new material.

Riama raneyi is recovered with moderate support as sister to a clade comprising *R. anatoloros* and a new species from the Amazonian slopes of the Ecuadorian Andes (purple clade; Figs 1–2). This group is strongly supported as sister to a clade containing *R. simotera* (O'Shaughnessy 1879), *R. colomaromani*, and two new species (including the cyan clade; Figs 1–2). Contrary to Torres-Carvajal et al. (2016) and Sánchez-Pacheco et al. (2018), our results place *R. cashcaensis* (Kizirian and Coloma 1991) as sister to *R. labionis* rather than *R. yumborum*, though this relationship is poorly supported.

We identified three geographically structured lineages within *Riama stigmatoral*, two of which are described as new species herein (lime green and yellow clades; Figs 1–2). We restrict *R. stigmatoral* to populations from the eastern Andean slopes of Morona Santiago province. This assignment is based on the holotype's morphology—specifically the dark brown venter with cream ventrolateral spotting—which matches Morona Santiago specimens but is absent in the other two lineages.

Similarly, *Riama unicolor* comprises three structured lineages, including two species described here (emerald green and red clades; Figs 1–2). We restrict the name *R. unicolor* to the inter-Andean valley populations of northern Ecuador (including the Quito valley). This decision is supported by the holotype's ventral scale count (24 transverse rows), which is consistent with inter-Andean populations but falls outside the range of the other two clades.

Morphological analyses: The MANOVA revealed significant interspecific morphological differences in Groups 1 and 3, primarily driven by cranial dimensions. In Group 1 (*Riama higginsi* sp. nov., *R. konstanti* sp. nov., and *R. unicolor*), frontonasal length (FNL; F=5.54, p=0.0072) and frontal length (FL; F=4.19, p=0.0217) varied significantly, while snout-vent length (SVL) did not (p=0.4183). Similarly, Group 3 (*R. tartetonorum* sp. nov. and *R. colomaromani*) showed significant variation only in FNL (F=4.66, p=0.0426). In both groups, caudal length (CL) showed only marginal significance (p≈0.06). In contrast, Group 2 (*R. stigmatoral*, *R. muchmoreorum* sp. nov., and *R. jenningsi* sp. nov.) appeared morphometrically homogeneous across all analyzed variables. These results suggest that head morphology is a more robust indicator of species differentiation in these taxa than body size (Table S4a, Fig. S4a).

K-means clustering of size-corrected variables identified varying optimal cluster numbers: four for Group 1 (s=0.539), six for Group 2 (s=0.415), and two for Group 3 (s=0.447; Fig. S4b). Principal Component Analysis (PCA) consistently identified head dimensions (FNL, FL) as the primary drivers of PC1 across all groups, explaining 35–38% of the total variance. Body proportions (SVL and CL) dominated PC2 and PC3, with the first three components cumulatively explaining 85–90% of the morphometric variance in all three groups (Table S4b, Fig. S4c).

Clustering of scale counts further supported group-specific structures. Silhouette values identified K=2 as the optimal cluster number for Group 1 (s=0.298), while K=3 provided the best fit for Group 2 (s=0.291) and Group 3 (s=0.272; Fig. S4d). Chi-square tests highlighted specific diagnostic traits for these clusters: Group 1 was differentiated by SPO, TRVS, and PPA; Group 2 by INL, LRDS, and TRVS; and Group 3 by TRDS, POC, and LTSR (Table S4c).

Multiple Correspondence Analysis (MCA) further identified the most influential lepidosis traits for species differentiation. In Group 1, femoral pore count (FP; 71.3%) and TRVS (48.0%) were the most significant contributors. In Group 2, lateral rows of dorsal scales (LRDS; 60.7%) and TRVS (49.4%) were most influential. For Group 3, LRDS showed the highest contribution (81.8%), followed by superciliaries (SPC; 56.8%). Across all groups, femoral pores and dorsal/ventral scale rows emerged as the most critical traits for defining morphological boundaries (Table S4d, Fig. S4e).

Systematic accounts: Species delimitation and the distinction between species-level and intraspecific variation remain complex challenges in systematic biology (Carstens et al. 2013; Burbrink et al. 2022). Following the General Lineage Species Concept (de Queiroz 2007), we restrict our species descriptions to lineages that are both monophyletic and possess diagnostic differences in coloration, lepidosis, and hemipenial morphology. Based on these integrative criteria, we here describe six new species of *Riama*.

***Riama higginsi* sp. nov.**
https://zoobank.org/84EC1000-18E7-449A-AB86-75D08762C50B
Figs 3, 4, 5a, 6

Type material. Holotype: TH 918 (Figs 3, 4a, 6), adult male collected by Alejandro Arteaga and Jose Vieira in 2020 at 23 km W of Chillogallo, Pichincha province, Ecuador (-0.27994, -78.69748; 2,391 m).

Figure 3: Dorsal and ventral views of the holotype of *Riama higginsi* sp. nov. TH 918.

Paratopotypes: TH 913, adult male; TH 915, subadult female; TH 916, adult male; TH 917, adult female; TH 919 (Fig. 4b), adult female; TH 920 (Fig. 4c), juvenile female; TH 921, subadult female; TH 922, adult female; TH 923 (Fig. 4d), juvenile female. See also Suppl. material 1.

Paratypes: KM 004 (Fig. 4e), adult male, Reserva Arlequín, Pichincha province, Ecuador (-0.02465, -78.72272; 2,097 m). See also Suppl. material 1.

Proposed English name: Higgins' Lightbulb Lizard.

Proposed Spanish name: Lagartija minadora de Higgins.

Diagnosis: *Riama higginsi* sp. nov. is placed in the genus *Riama*, as diagnosed by Doan & Castoe (2005), based on phylogenetic evidence (Fig. 1). The species is diagnosed based on the following combination of characters: (1) frontonasal 0.9–1.2 × longer than frontal; (2) nasoloreal

suture absent; (3) supraoculars 4–5, usually four, with 2nd in contact with ciliaries; (4) supraciliary series incomplete, usually two (range 2–4; complete in holotype on the right side); (5) supralabial-subocular fusion absent; (6) postoculars usually two; (7) postparietals three; (8) supratympanic temporals three; (9) genials two, transverse sutures not perpendicular with respect to midline of body; (10) dorsals rectangular, juxtaposed, striated/keeled; (11) longitudinal dorsal scale rows in males 21–22, in females 20–22; (12) transverse dorsal scale rows in males 35–36, in females 33–36; (13) transverse ventral scale rows in males 21–23, in females 20–22; (14) lateral scale rows 1; (15) femoral pores per leg in males 11–12, in females 1; (16) subdigital scales on Toe I 4–6; (17) limbs not overlapping when adpressed against body in adults; (18) anterior cloacal plate scales paired; (19) hemipenis capitate; hemipenial body nude, lacking flounces on both sulcate and asulcate views, with a series of markedly reduced oblique rows of flounces on the distal half of the hemipenial body on the lateral side; flounces without evident spinules; (20) dorsum of adult males and females brown with scattered irregular black spots and a black-bordered ochraceous dorsolateral stripe running from the neck to the first third of the body; lips blackish with irregular white bars or spots; belly and chin uniformly shiny black, with irregular red blotches on the throat; lower flanks, sides of tail, and limbs of adult males with a reddish tint; ventral surface of tail bearing irregular reddish stripes on a black background; (21) 52–53 mm SVL in males, 52–55 mm in females.

Comparisons: *Riama higginsi* sp. nov. resembles *R. unicolor* in size, coloration, and lepidosis, but it differs from this species by being more slender, smaller in SVL, flounces not converging on the asulcate view of the hemipenial body (asulcate expansion pleat present), having no clearly defined black stripes on the tail underside (Fig. 5), a lower number of transverse rows of ventral scales (21–22 vs. 23–25), a higher number of supraoculars (4 vs. 2–3), and a lower number of transverse rows of dorsal scales (33–36 vs. 37–43). The new species further differs from all other congeners (for which hemipenial morphology is known) in lacking calcified spines on the hemipenial flounces. From *R. antioquensis* and *R. columbiana*, it differs by having fewer than 40 transverse dorsal scale rows. From *R. labionis* and *R. yumborum*, it differs by having a uniformly black belly. From *R. konstanti* sp. nov., the new species differs by being smaller in SVL, having a lower number of transverse rows of ventral scales (21–22 vs. 23–26), and by having a clearly defined black-bordered ochraceous dorsolateral stripe running from the neck to the first third of the body. From *R. anatoloros*, *R. balneator*, *R. ellasabinae* sp. nov., *R. simotera*, and *R. striata*, the new species differs by having an incomplete series of supraciliary scales. From *R. cashcaensis*, *R. jenningsi* sp. nov., *R. muchmoreorum* sp. nov., *R. orcesi*, and *R. stigmatoral*, it differs by having femoral pores in females. From *R. colomaromani* and *R. tarletonorum* sp. nov., it differs by being smaller in SVL and by lacking black coloration in adult males. From *R. cashcaensis*, it further differs by having a higher number of supratympanic temporals (3 vs. 2) as well as by lacking a ventral pattern of transverse bands. From *R. meleagris* and *R. raneyi*, it differs by having more than one supraciliary scale.

Hemipenial morphology: Based on the organs of TH 918 (Fig. 6) and KM 004. The hemipenial body is nearly columnar, tapered toward the base, ending in two

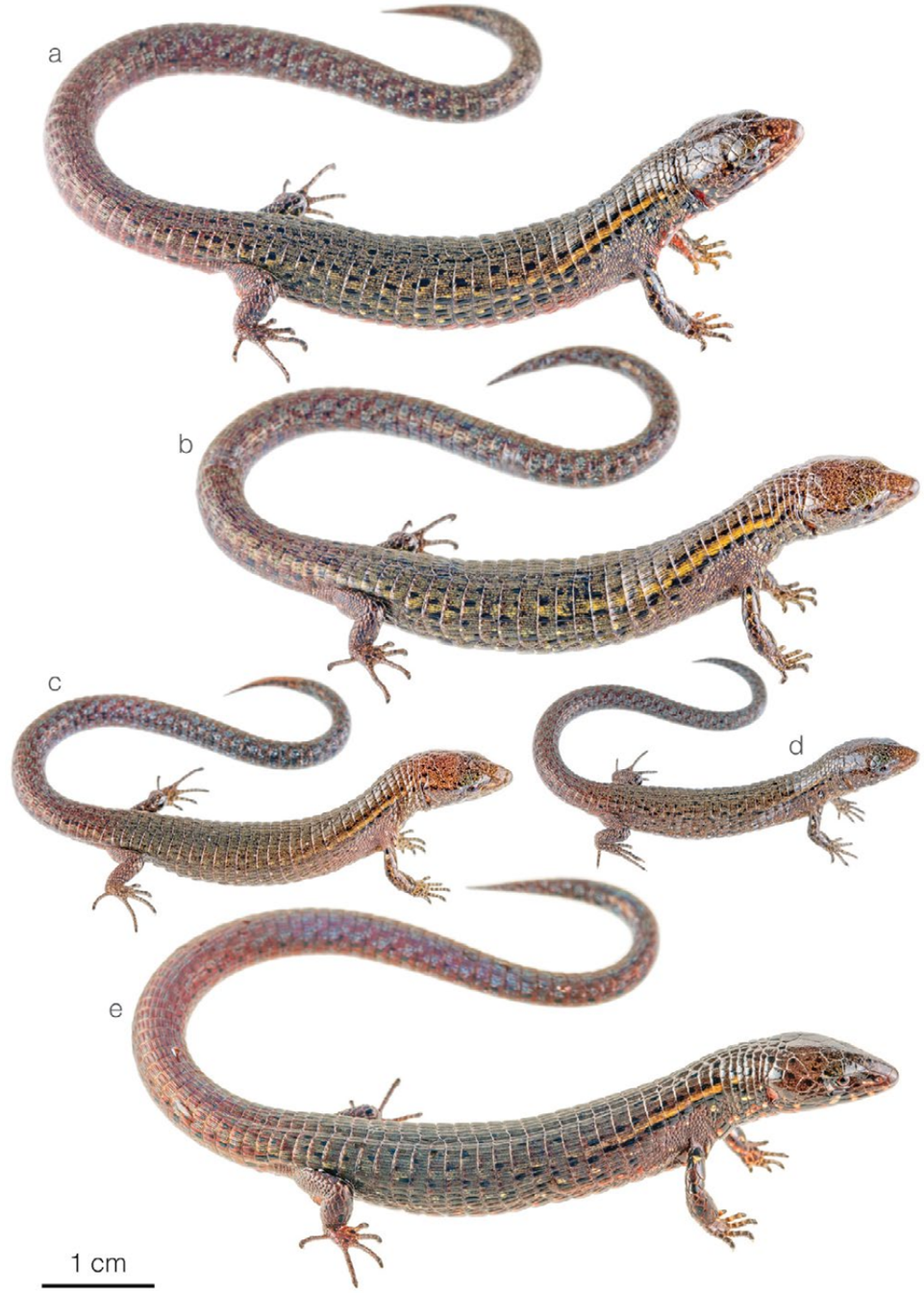

Figure 4: Specimens of *Riama higginsi* sp. nov. in life: (a) TH 918 adult male holotype; (b) TH 919 adult female paratopotype; (c) TH 920 juvenile female paratopotype; (d) TH 923 juvenile female paratopotype; (e) KM 004 adult male from Arlequín Reserve, Pichincha province.

Figure 5: Ventral coloration in three species of *Riama* in life: (a) black belly and red tail underside with broken lines in *R. higginsi* sp. nov. KM 004; (b) melanistic ventral surfaces in *R. konstanti* sp. nov.; (c) black belly and red tail with continuous longitudinal stripes in *R. unicolor*.

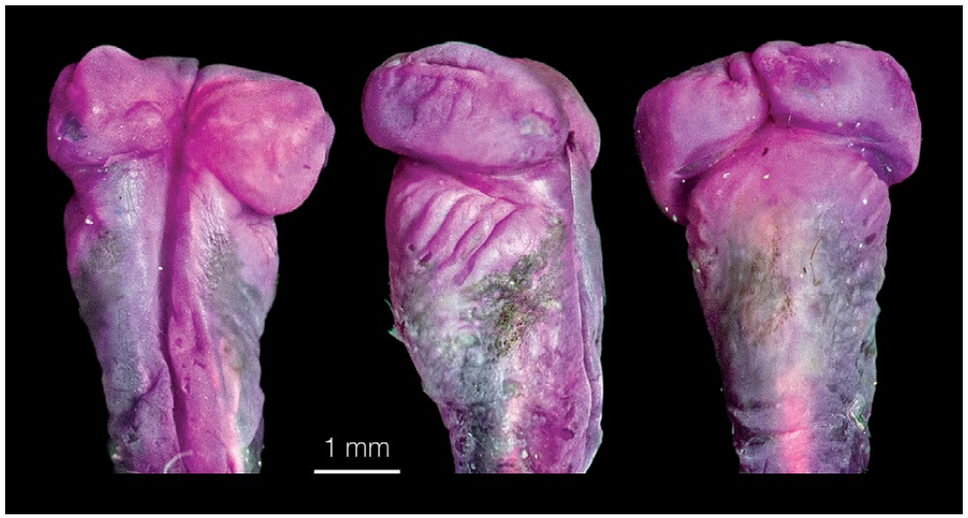

Figure 6: Hemipenial architecture of *Riama higginsi* sp. nov. TH 918 holotype in sulcate, lateral, and asulcate views.

symmetric small and partially everted (in KM 004) or fully everted (TH 918) lobes outlined by folds; a deep sulcus spermaticus, central in position, originates at the base of the organ and proceeds in a straight line towards the lobes. The sulcus spermaticus consists of a single channel emarginated by lobular folds and ending in a barely discernible bifurcation at the head. The sulcus spermaticus is bordered on each side by a wide nude area along the entire sulcate view. A series of 5–6 short rows of oblique flounces bearing barely discernible comb-like spicules is evident on the distal portion of the hemipenial body on the lateral side. The rows of flounces do not converge on the asulcate surface, which is nude (asulcate expansion pleat present).

Description of holotype: Adult male, SVL 53 mm, tail length 90 mm; head scales smooth to slightly rugose; rostral wider than long, higher than adjacent supralabials, in contact posteriorly with nasal, frontonasal, and anteriormost supralabials; frontonasal widest near the posterior suture, in contact laterally with nasals and posteriorly with frontal and anteriormost supraoculars; prefrontals absent; frontal longer than wide, widest anteriorly, anterior suture straight, lateral sutures nearly straight, posterior suture angular with point directed posteriorly, in contact with first and second supraoculars laterally and frontoparietals posteriorly; frontoparietals pentagonal, in contact with second and third supraoculars laterally on the left side, in contact with second, third, and fourth supraoculars laterally on the right side, parietals posterolaterally, and interparietal posteromedially; interparietal long, heptagonal, and with slightly concave lateral sutures, in contact with parietals laterally and postparietals posteriorly; parietals hexagonal, in contact with third and fourth supraoculars anterolaterally on the left side, in contact with fourth and fifth supraoculars anterolaterally on the right side, dorsalmost temporals posterolaterally, and postparietals posteriorly; postparietals three (two small scales embedded between the postparietal scales), external longest laterally; supraoculars four on left side and five on right side, with second in contact with ciliaries on the right side; nasoloreal suture absent; superciliaries four on left side and two on right side; palpebral disc semitransparent and divided into three large unpigmented scales; frenocular nearly trapezoidal in shape, in contact with nasal anteriorly; six circumorbitals between posteriormost supraocular and frenocular; postoculars three; temporals smooth to slightly rugose; supratympanic temporals three on each side; supralabials seven; infralabials five; mental wider than long, in contact with anteriormost infralabials laterally and postmental posteriorly; postmental pentagonal, posterior suture angular, with angle directed posteriorly, in contact with first and second infralabials laterally; genials in two pairs, anteriormost pair trapezoidal, in contact with second and third infralabials; posterior pair roughly hexagonal, in contact with third infralabials; scale rows between genials and collar fold (along midventral line) nine; medialmost scales of posteriormost scale row distinctly enlarged, smooth to slightly rugose; posteriormost gular row enfolded posteriorly; lateral neck scales squarish or rounded, smooth.

Natural history: *Riama higginsi* sp. nov. occurs in well-preserved montane cloud forests as well as in forest-edge situations along dirt roads. Most of the type series (10 of 11 individuals) was found hidden under rocks, moss, roots, and in crevices in rocky walls besides dirt roads adjacent

to forested steep slopes. KM 004 was buried under dry soft soil among roots in a dirt wall beside a trail, living syntopically with *Lepidoblepharis conolepis*. Two specimens were hidden under the mossy surface of a cliff that had water running through it in the form of a small waterfall. A clutch of two eggs was found beside these two adults. One individual (not collected) was found hidden beneath the moss of a tree, 4 m above the ground. Cisneros-Heredia (2005) reports a "*Proctoporus* cf. *unicolor*" (probably *Riama higginsi* sp. nov.) in the stomach of a *Saphenophis boursieri* from the Río Guajalito reserve.

Distribution: *Riama higginsi* sp. nov. is known from at least 13 localities (listed under Suppl. material 3) along the western foothills of the Ecuadorian Andes in Pichincha and Santo Domingo de los Tsáchilas provinces. The species occurs over an area of approximately 569 km² and has been recorded at elevations of 1,734–2,391 m above sea level (Fig. 2).

Etymology: This new species of lizard is named after Joseph Higgins, whose dedication to the preservation of tropical biodiversity is exemplary. Higgins' support of the Khamai Foundation has helped this young organization protect 186 hectares of cloud forest and rainforest ecosystems in Ecuador, including key habitat for the survival of *Riama higginsi* sp. nov.

Conservation status: We consider this species to be in the Near Threatened conservation category following the IUCN criteria (IUCN 2012) because it has been recorded in more than 10 localities (listed in Suppl. material 3) and is distributed over an area which retains most of its original cloud forest cover (MAE 2012). Therefore, the species is considered to face no major immediate extinction threats.

***Riama konstanti* sp. nov.**
https://zoobank.org/29D26D82-80E9-4B5F-89E0-9C3F2659FF7C
Figs 5b, 7, 8

Type material. Holotype: TH 896 (Figs 7, 8d), subadult male collected by Jose Vieira, Amanda Quezada, Frank Pichardo, Harry Turner, and Carlos Nivelo in 2020 at Otonga Reserve, Cotopaxi province, Ecuador (-0.41631, -79.00631; 2,142 m).

Paratopotypes: TH 848, adult female; TH 858, subadult female; TH 860 (Fig. 8a), juvenile male; TH 861, juvenile female; TH 862, juvenile female; TH 863, adult male; TH 874, juvenile male; TH 891, adult female; TH 892, adult male; TH 893, adult male; TH 894 (Fig. 8b), juvenile male. See also Suppl. material 1.

Paratypes: TH 759, adult male; TH 760, juvenile female; TH 761 (Fig. 8c), adult female. All three from 9 km S of Las Pampas, Cotopaxi province, Ecuador (-0.48750, -78.99389; 2,134 m). See also Suppl. material 1.

Figure 7: Dorsal and ventral views of the holotype of *Riama konstanti* sp. nov. TH 896.

Figure 8: Photographs of some specimens of *Riama konstanti* sp. nov. in life: (a) TH 860 juvenile male from the type locality; (b) TH 894 juvenile male from the type locality; (c) TH 761 adult female from 9 km S of Las Pampas, Cotopaxi province; (d) TH 896 adult male holotype.

Proposed English name: Konstant's Lightbulb Lizard.

Proposed Spanish name: Lagartija minadora de Konstant.

Diagnosis: *Riama konstanti* sp. nov. is placed in the genus *Riama*, as diagnosed by Doan & Castoe (2005), based on phylogenetic evidence (Fig. 1). The species is diagnosed based on the following combination of characters: (1) frontonasal 0.9–1.1 × longer than frontal; (2) nasoloreal suture absent; (3) supraoculars four, with 2nd or 2nd and 3rd in contact with ciliaries; (4) supraciliary series incomplete, usually two (TH 848 has three); (5) supralabial-subocular fusion absent; (6) postoculars usually two; (7) postparietals three; (8) supratympanic temporals three; (9) genials two, transverse sutures nearly perpendicular with respect to midline of body; (10) dorsals rectangular, juxtaposed, striated/keeled; (11) longitudinal dorsal scale rows in both males and females 20–22; (12) transverse dorsal scale rows in males 35–37, in females 34–39; (13) transverse ventral scale rows in both males and females 20–22; (14) lateral scale rows 1–2; (15) femoral pores per leg in males 10–14, in females 1; (16) subdigital scales on Toe I 4–5; (17) limbs not overlapping when adpressed against body in adults; (18) anterior cloacal plate scales paired; (19) hemipenis capitate; hemipenial body nude, lacking flounces on both sulcate and asulcate surfaces, with a series of five markedly reduced oblique rows of flounces on the distal half of the hemipenial body on the lateral side; flounces without evident spinules; (20) dorsum of adult males and females uniformly brown with scattered irregular black and cream speckling; lips blackish with irregular cream spots; belly uniformly shiny black (sutures between ventral scales cream in juveniles), becoming brownish on the throat, which may enclose irregular cream markings; lower flanks, sides of tail, and limbs with a reddish tint that is more intense on adult males; ventral surface of tail in adult males bearing reddish stripes on a black background; ventral surface of tail in adult females heavily obscured by black pigment; (21) 54.5–62 mm SVL in males, 53–57 mm in females.

Comparisons: *Riama konstanti* sp. nov. resembles *R. unicolor* in size, coloration, and lepidosis, but it differs from this species by having a lower number of transverse rows of ventral scales (20–22 vs. 23–25), a higher number of supraoculars (4 vs. 2–3), and by having an expansion pleat preventing the flounces from converging on the asulcate view of the hemipenial body. The new species further differs from all other congeners (for which hemipenial morphology is known) in lacking calcified spines on the hemipenial flounces. From *R. antioquensis* and *R. columbiana*, it differs by having fewer than 40 transverse dorsal scale rows. From *R. labionis* and *R. yumborum*, it differs by having a uniformly black belly. From *R. higginsi* sp. nov., the new species differs by being larger in SVL, having a higher number of transverse rows of ventral scales (23–26 vs. 21–22), and by lacking a clearly defined black-bordered ochraceous dorsolateral stripe running from the neck to the first third of the body. From *R. anatoloros*, *R. balneator*, *R. ellasabinae* sp. nov., *R. simotera*, and *R. striata*, the new species differs by having an incomplete series of supraciliary scales. From *R. cashcaensis*, *R. jenningsi* sp. nov., *R. muchmoreorum* sp. nov., *R. orcesi*, and *R. stigmatoral*, it differs by having femoral pores in females. From *R. colomaromani* and *R. tarletonorum* sp. nov., it differs by being smaller in SVL and by lacking black coloration in adult males. From *R. cashcaensis*, it further differs by having a higher number of supratympanic temporals (3 vs. 2) as well as by lacking a ventral pattern of transverse bands. From *R. meleagris* and *R. raneyi*, it differs by having more than one supraciliary scale.

Hemipenial morphology: Based on the poorly everted organ of TH 896. The hemipenial body is nearly columnar, tapered toward the base, ending in two symmetric small and partially everted lobes outlined by folds; a deep sulcus spermaticus, central in position, originates at the base of the organ and proceeds in a straight line towards the lobes. The sulcus spermaticus consists of a single channel emarginated by lobular folds and ending in a barely discernible bifurcation at the head. The sulcus spermaticus is bordered on each side by a wide nude area along the entire sulcate view. A series of five short rows of oblique flounces bearing no discernible spicules is evident on the distal portion of the hemipenial body on the lateral side. The rows of flounces do not converge on the asulcate surface, which is nude (asulcate expansion pleat present).

Description of holotype: Male, SVL 54.5 mm, tail (incomplete) length 75 mm; head scales smooth to slightly rugose; rostral wider than long, higher than adjacent supralabials, in contact posteriorly with nasal, frontonasal, and anteriormost supralabials; frontonasal rounded trapezoidal in shape, widest near the posterior suture, in contact laterally with nasals and posteriorly with frontal, anteriormost supraoculars, and anteriormost supraciliaries; prefrontals absent; frontal longer than wide, widest anteriorly, anterior suture straight, lateral sutures straight, posterior suture angular with point directed posteriorly, in contact with first and second supraoculars laterally and frontoparietals posteriorly; frontoparietals pentagonal, in contact with second and third supraoculars laterally, parietals posterolaterally, and interparietal posteromedially; interparietal long, heptagonal, and with slightly concave lateral sutures, in contact with parietals laterally and postparietals posteriorly; parietals pentagonal, in contact with third and fourth supraoculars anterolaterally, upper temporals posterolaterally, and postparietals posteriorly; postparietals three, external longest laterally; supraoculars four with second in contact with ciliaries; nasoloreal suture absent; superciliaries two; palpebral disc semitransparent and divided into four large unpigmented scales; frenocular nearly trapezoidal in shape, in contact with nasal anteriorly; five circumorbitals between posteriormost supraocular and frenocular; postoculars two; temporals smooth; supratympanic temporals three; supralabials six; infralabials four; mental wider than long, in contact with anteriormost infralabials laterally and postmental posteriorly; postmental pentagonal, posterior suture angular, with angle directed posteriorly, in contact with first and second infralabials laterally; genials in two pairs, anteriormost pair trapezoidal, in contact with second and third infralabials; posterior pair roughly pentagonal, in contact with third and fourth infralabials; scale rows between genials and collar fold (along midventral line) nine; medialmost scales of posteriormost scale row distinctly enlarged, smooth; posteriormost gular row enfolded posteriorly; lateral neck scales squarish or rounded, barely striated.

Natural history: *Riama konstanti* sp. nov. occurs in well-preserved montane cloud forests as well as in forest-edge situations along dirt roads. At 9 km S of Las

Pampas, three individuals were found hidden under soft soil and damp leaf-litter in remnants of native forest near pastures. At Otonga Reserve, individuals were uncovered by digging in areas of soft soil on slopes within primary forest.

Distribution: *Riama konstanti* sp. nov. is known from just two localities along the western foothills of the Ecuadorian Andes in Cotopaxi province. The species occurs over an area of approximately 5 km² and has been recorded at elevations of 2,100–2,142 m above sea level (Fig. 2).

Etymology: This species is named after William "Bill" Konstant in recognition of his more than four decades of contributions to wildlife conservation. Since 1980, he has helped safeguard populations of threatened species and their habitats in Latin America, Africa, and Asia.

Conservation status: We consider *Riama konstanti* sp. nov. to be Critically Endangered following IUCN Red List criteria B2a, b (i, iii, iv) (IUCN 2012) because the species is known only from an extremely small (around 5 km²) cloud forest area that continues to decline in extent and quality due to deforestation. Only two localities are known; they lack connectivity between them, and one is under immediate threat of disappearance due to the expansion of the cattle grazing frontier.

***Riama jenningsi* sp. nov.**
https://zoobank.org/6C10985B-FFF4-474C-899E-F5D26DEBFE62
Figs 9, 10, 11

Type material. Holotype: TH 477 (Figs 9, 10d), adult male collected by Jose Vieira and Amanda Quezada in 2020 at Guachapala, Azuay province, Ecuador (-2.78224, -78.71705; 2,595 m).

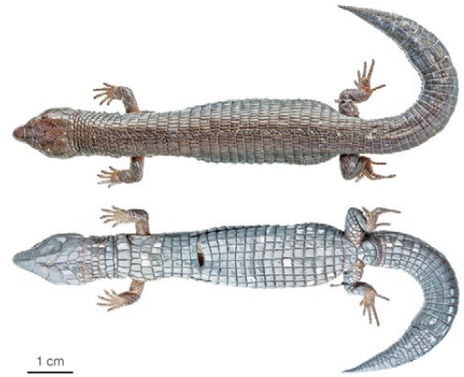

Figure 9: Holotype of *Riama jenningsi* sp. nov. TH 477 in dorsal and ventral view.

Paratopotypes: TH 443, adult female; TH 444 (Fig. 10c), juvenile male; TH 445, adult male; TH 447, adult female; TH 452, adult male; TH 476, adult female. See also Suppl. material 1.

Paratypes: TH 300, adult male; TH 301, adult female; TH 302 (Fig. 10a), adult female; TH 303, adult female; TH 304, juvenile female; TH 305, subadult male; TH 306, adult female; TH 307, juvenile male. All eight from Santa Ana, Azuay province, Ecuador (-2.93236, -78.92710; 2,558 m). See also Suppl. material 1.

Proposed English name: Jennings' Lightbulb Lizard

Proposed Spanish name: Lagartija minadora de Jennings

Diagnosis: *Riama jenningsi* sp. nov. is placed in the genus *Riama*, as diagnosed by Doan & Castoe (2005), based on phylogenetic evidence (Fig. 1). The species is diagnosed based on the following combination of characters: (1) frontonasal 1–1.4 × longer than frontal; (2) nasoloreal suture incomplete or absent; (3) supraoculars

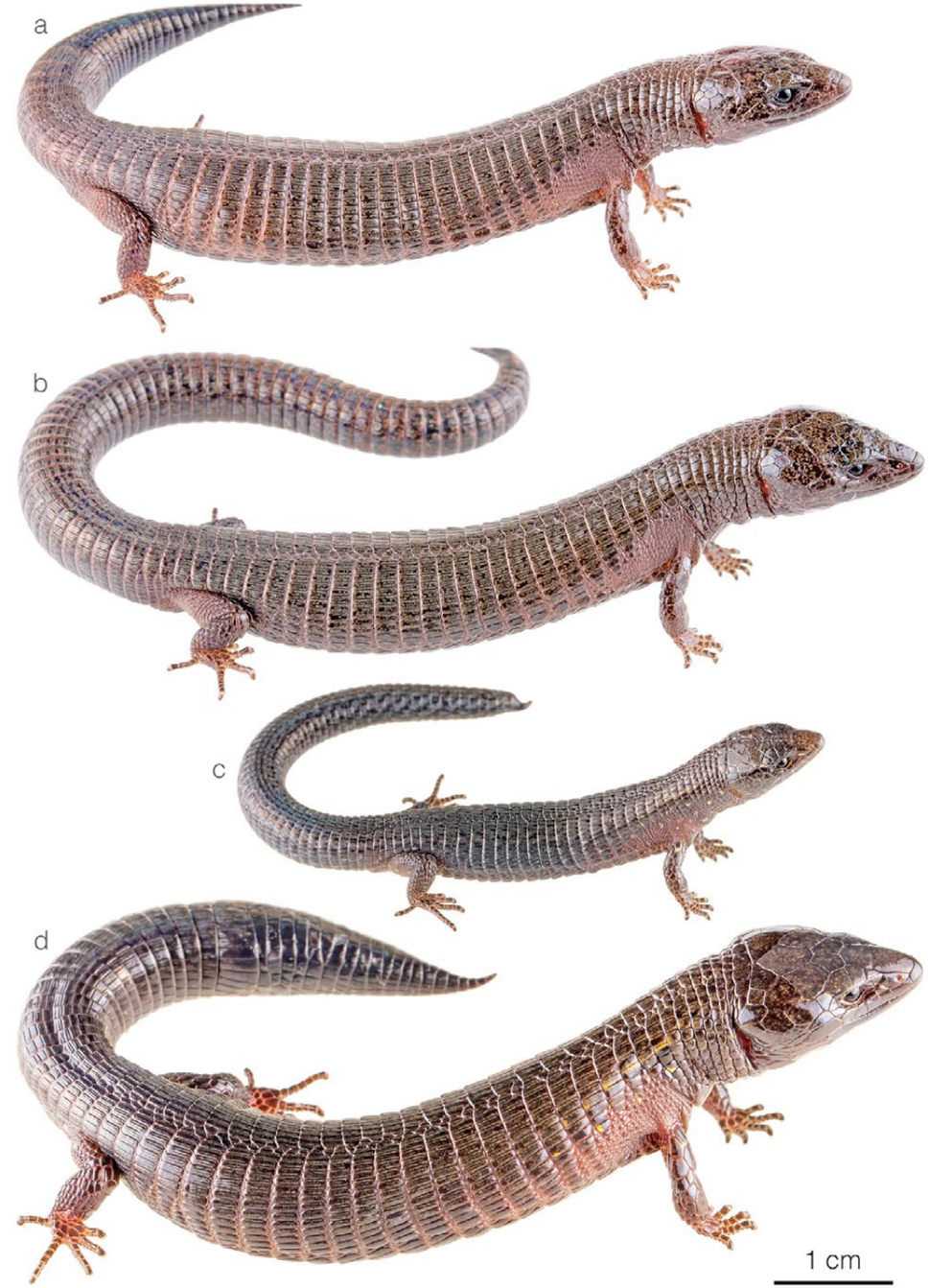

Figure 10: Photographs of some specimens of *Riama jenningsi* sp. nov. in life: (a) TH 302 adult female from Santa Ana, Azuay province; (b) adult male from Santa Ana, Azuay province; (c) TH 444 juvenile male from the type locality; (d) TH 477 adult male holotype.

four, with 2nd and sometimes 3rd in contact with ciliaries; (4) supraciliary series incomplete, one anteriorly, one posteriorly; (5) supralabial-subocular fusion absent; (6) postoculars two; (7) postparietals usually two; (8) supratympanic temporals usually three; (9) genials two or three, with transverse sutures nearly perpendicular with respect to midline of body; (10) dorsals rectangular, juxtaposed, striated/keeled; (11) longitudinal dorsal scale rows in both males and females 22–27; (12) transverse dorsal scale rows in males 37–39, in females 38–43; (13) transverse ventral scale rows in both males and females 22–24; (14) lateral scale rows 1–2; (15) femoral pores per leg in males 7–10, in females 0; (16) subdigital scales on Toe I usually 5; (17) limbs not overlapping when adpressed against body in adults; (18) anterior cloacal plate scales typically divided into two or into four, with two larger inner plates accompanied by two smaller outer plates; (19) hemipenis capitate; flounces bearing comb-like spinules on the asulcate surface, forming W-shaped chevrons; asulcate expansion pleat absent; (20) dorsum of adult males and females uniformly dark brown with fine black speckling and with scattered yellow spots dorsolaterally on some adults; ventral surfaces uniformly shiny black without spots or blotches; (21) 61–79.9 mm SVL in males, 60–70 mm in females.

Comparisons: *Riama jenningsi* sp. nov. resembles *R. stigmatoral* in size, coloration, and lepidosis, from which it differs by having a shiny black belly without bright reddish, orange, or cream spots along the flanks, and by having fewer than 12 longitudinal ventral scale rows. From *R. muchmoreorum* sp. nov., it differs by having a uniformly black or dark brown belly (vs. checkerboard ventral pattern), a higher number of transverse dorsal scale rows, a comparatively longer frontonasal, and by having a nasoloreal suture in some individuals. From *R. antioquensis*, it differs by lacking prefrontal scales. From *R. columbiana*, it differs by having a uniform black belly and fewer than three lateral scale rows. From *R. cashcaensis*, it differs by having a uniform black belly without light transverse bands or blotches and by having more than one supraciliary scale. From *R. higginsi* sp. nov., *R. konstanti* sp. nov., *R. labionis*, *R. unicolor*, and *R. yumborum*, it differs by being larger in SVL, having pale cream blotches instead of thin reddish stripes on the tail underside, and by lacking femoral pores in females. From *R. anatoloros*, *R. balneator*, *R. ellasabinae* sp. nov., *R. orcesi*, *R. simotera*, and *R. striata*, the new species differs by having an incomplete series of supraciliary scales. From *R. colomaromani* and *R. tarletonorum* sp. nov., it differs by having a higher number of transverse ventral scale rows, lacking femoral pores in females, and lacking white spots along the flanks. From *R. meleagris* and *R. raneyi*, it differs by having more than one supraciliary scale.

Hemipenial morphology: Based on the organ of TH 477 (Fig. 11). The hemipenial body is nearly columnar, tapered toward the base, ending in two symmetric small and partially everted lobes outlined by folds; a deep sulcus spermaticus, central in position, originates at the base of the organ and proceeds in a straight line towards the lobes. The sulcus spermaticus consists of a single channel emarginated by lobular folds with no discernible bifurcation at the head. The sulcus spermaticus is bordered on each side by a narrow nude area flanked by six rows of oblique flounces. The flounces cover the distal half of the hemipenial body on both lateral and asulcate views, where they

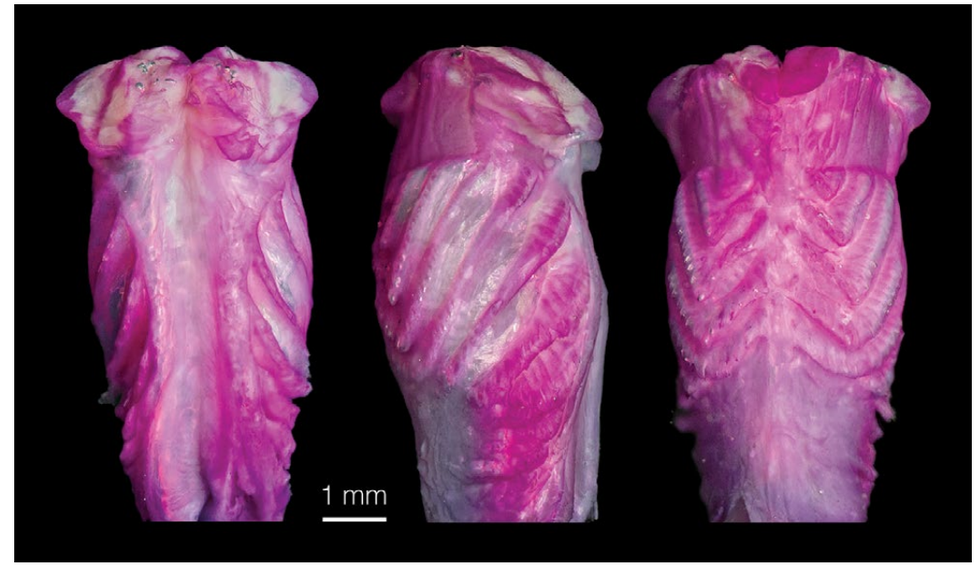

Figure 11: Hemipenial architecture of *Riama jenningsi* sp. nov. TH 477 holotype in sulcate, lateral, and asulcate views.

bear comb-like spicules. The flounces are arranged in W-shaped rows nearly continuous along the asulcate surface (expansion pleat absent) extending to the borders of each nude area contiguous to the sulcus spermaticus.

Description of holotype: Male, SVL 79.9 mm, tail length 56.0 mm; head scales smooth; rostral wider than long, higher than adjacent supralabials, in contact posteriorly with nasal, frontonasal, and anteriormost supralabials; frontonasal rounded trapezoidal in shape, widest near the posterior suture, in contact laterally with nasals and posteriorly with frontal, anteriormost supraoculars, and anteriormost supraciliaries; prefrontals absent; frontal about as long as wide, widest anteriorly, with lateral sutures slightly concave, posterior suture angular with point directed posteriorly, in contact with first and second supraoculars laterally and frontoparietals posteriorly; frontoparietals pentagonal, in contact with second and third supraoculars laterally, parietals posterolaterally, and interparietal posteromedially; interparietal long, hexagonal, and with straight lateral sutures, in contact with parietals laterally and postparietals posteriorly; parietals polygonal, in contact with third and fourth supraoculars anterolaterally, dorsalmost temporals posterolaterally, and postparietals posteriorly; postparietals two, longest laterally, with the left one fused with the dorsalmost temporal; supraoculars four with second and third in contact with ciliaries on the right side and with second in contact with ciliaries on the left side; nasoloreal suture absent; superciliaries two; palpebral disc semitransparent and divided into three large unpigmented scales; frenocular nearly trapezoidal in shape, in contact with nasal anteriorly; six circumorbitals between posteriormost supraocular and frenocular; postoculars two; temporals smooth; supratympanic temporals 3/3;

supralabials seven; infralabials five; mental wider than long, in contact with anteriormost infralabials laterally and postmental posteriorly; postmental rounded trapezoidal in shape, posterior suture angular, with angle directed posteriorly, in contact with first and second infralabials laterally; genials in two pairs, anteriormost pair trapezoidal, in contact with second and third infralabials; posterior pair polygonal, in contact with third and fourth infralabials; scale rows between genials and collar fold (along midventral line) ten, with the posteriormost scale row distinctly enlarged, smooth; posteriormost gular row enfolded posteriorly; lateral neck scales rounded, smooth.

Natural history: *Riama jenningsi* sp. nov. has only been recorded in agricultural landscapes consisting of a matrix of pastures, crops, living fences, and remnants of native vegetation. At the type locality, individuals were found under rocks, logs, dirt clods, as well as in crevices in dirt walls along roads. As many as four individuals were found under the same stone, alongside clutches of two eggs. At Santa Ana, Azuay province, individuals were found under surface objects in pastures.

Distribution: *Riama jenningsi* sp. nov. is known from seven localities along the watershed of the Río Paute in Azuay and Cañar provinces, southeastern Ecuador. The species occurs over an area of approximately 226 km² and has been recorded at elevations of 2,487–3,044 m above sea level (Fig. 2).

Etymology: The specific epithet *jenningsi* is a patronym honoring Walter Jennings, a tireless conservationist and naturalist who supports and served on the board of the Jocotoco Foundation. Walt and his wife Linda were among the most important early supporters of Alejandro's work on biodiversity and conservation. Most of the new lizard species described in this work are now in the process of being protected thanks to the Jennings.

Conservation status: We consider *Riama jenningsi* sp. nov. to be Endangered following IUCN Red List criteria B2a, b (i, iii, iv) (IUCN 2012) because the species is known only from a small (here estimated to be under 500 km²) area of forest patches that continues to decline in extent and quality due to the expansion of the agricultural frontier. Only seven localities are known; they lack connectivity between them and none of them are protected.

***Riama muchmoreorum* sp. nov.**
https://zoobank.org/1F1294C4-0914-49BC-85C1-AFA3365F68FF
Figs 12, 13

Type material. Holotype: TH 501 (Figs 12, 13a), subadult male collected by Jose Vieira and Amanda Quezada in 2020 at Zhoray–Mazar road, Cañar province, Ecuador (-2.54645, -78.69112; 2,765 m).

Paratopotypes: TH 367, subadult female; TH 368 (Fig. 13d), adult female; TH 369

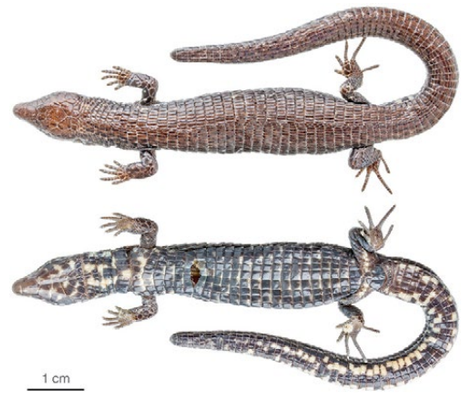

Figure 12: Dorsal and ventral views of the holotype of *Riama muchmoreorum* sp. nov.

Figure 13: Photographs of some specimens of *Riama muchmoreorum* sp. nov. in life: (a) TH 501 adult male holotype; (b) TH 371 juvenile male from the type locality; (c) TH 369 adult female from the type locality; (d) TH 368 adult female from the type locality.

(Fig. 13c), adult female; TH 370, adult female; TH 371 (Fig. 13b), juvenile male; TH 372, subadult male; TH 373, adult female; TH 374, subadult female; TH 377, subadult male; TH 378, subadult female; TH 379, juvenile female. See also Suppl. material 1.

Proposed English name: Muchmores' Lightbulb Lizard.

Proposed Spanish name: Lagartija minadora de los Muchmore.

Diagnosis: *Riama muchmoreorum* sp. nov. is placed in the genus *Riama*, as diagnosed by Doan & Castoe (2005), based on phylogenetic evidence (Fig. 1). The species is diagnosed based on the following combination of characters: (1) frontonasal 0.9–1.2 × longer than frontal; (2) nasoloreal suture absent; (3) supraoculars four, with 2nd and 3rd in contact with ciliaries; (4) supraciliary series incomplete, one anteriorly, one posteriorly; (5) supralabial-subocular fusion absent; (6) postoculars two; (7) postparietals usually two; (8) supratympanic temporals usually three; (9) genials two, transverse sutures nearly perpendicular with respect to midline of body; (10) dorsals rectangular, juxtaposed, striated/keeled; (11) longitudinal dorsal scale rows in males 23–24, in females 23–25; (12) transverse dorsal scale rows in males 37, in females 37–39; (13) transverse ventral scale rows in males 22–24, in females 22–23; (14) lateral scale rows 1–2; (15) femoral pores per leg in males 6–9, in females 0; (16) subdigital scales on Toe I 5–6; (17) limbs not overlapping when adpressed against body in adults; (18) anterior cloacal plate scales typically divided into two or into four, with two larger inner plates accompanied by two smaller outer plates; (19) hemipenial morphology unknown; (20) dorsum of adult males and females uniformly dark brown with scattered bright yellowish spots along the lower flanks; lower flanks of adult males bedecked with bright orange or reddish blotches; lips dark brown with irregular yellowish-white spots; ventral surfaces uniformly shiny black with broad cream to orangish irregular blotches, forming a checkerboard pattern in some individuals; (21) 52–65 mm SVL in males, 52–80 mm in females.

Comparisons: *Riama muchmoreorum* sp. nov. can be distinguished from all congeners except *R. cashcaensis* by having a checkerboard ventral pattern. This new species resembles *R. stigmatoral* in size, coloration, and lepidosis, from which it differs by having a checkerboard ventral pattern (instead of dark brown with spots along the flanks), lacking a nasoloreal suture, and by having a lower number of femoral pores per leg in males (6–9 vs. 9–11). From *R. jenningsi* sp. nov., it differs by having a checkerboard ventral pattern (instead of uniformly black or dark brown), a lower number of transverse dorsal scale rows, a comparatively shorter frontonasal, and by lacking a nasoloreal suture (vs. nasoloreal suture present in some individuals of *R. jenningsi* sp. nov.). From *R. antioquensis* and *R. columbiana*, it differs by having fewer than 40 transverse dorsal scale rows. From *R. cashcaensis*, it differs by having three supratympanic temporals and more than one supraciliary scale. From *R. higginsi* sp. nov., *R. konstanti* sp. nov., *R. labionis*, *R. unicolor*, and *R. yumborum*, it differs by being larger in SVL, having pale cream blotches instead of thin reddish stripes on the tail underside, and by lacking femoral pores in females. From *R. anatoloros*, *R. balneator*, *R. ellasabinae* sp. nov., *R. orcesi*, *R. simotera*, and *R. striata*, the new species differs by having an incomplete series of supraciliary scales. From *R. colomaromani* and *R. tarletonorum* sp. nov., it differs by having a higher number of transverse ventral scale rows, lacking femoral pores in females, and having a blotched tail underside. From *R. meleagris* and *R. raneyi*, it differs by having more than one supraciliary scale.

Description of holotype: Male, SVL 65.32 mm, tail length 65.8 mm; head scales smooth; rostral wider than long, higher than adjacent supralabials, in contact posteriorly with nasal, frontonasal, and anteriormost supralabials; frontonasal rounded trapezoidal in shape, widest near the posterior suture, in contact laterally with nasals and posteriorly with frontal, anteriormost supraoculars, and anteriormost supraciliaries; prefrontals absent; frontal longer than wide, widest anteriorly, with lateral sutures slightly concave, posterior suture angular with point directed posteriorly, in contact with first and second supraoculars laterally and frontoparietals posteriorly; frontoparietals pentagonal, in contact with the third supraocular laterally, parietals posterolaterally, and interparietal posteromedially; interparietal long, hexagonal, and with slightly concave lateral sutures, in contact with parietals laterally and postparietals posteriorly; parietals polygonal, in contact with third and fourth supraoculars anterolaterally, dorsalmost temporals posterolaterally, and postparietals posteriorly; postparietals two, longest laterally; supraoculars four, with second and third in contact with ciliaries; nasoloreal suture absent; superciliaries two; palpebral disc semitransparent and divided into four large unpigmented scales; frenocular nearly trapezoidal in shape, in contact with nasal anteriorly; five circumorbitals between posteriormost supraocular and frenocular on the left side and six circumorbitals between posteriormost supraocular and frenocular on the right side; postoculars two; temporals smooth; supratympanic temporals 3/3; supralabials seven; infralabials four; mental wider than long, in contact with anteriormost infralabials laterally and postmental posteriorly; postmental hexagonal, posterior suture angular, with angle directed posteriorly, in contact with first and second infralabials laterally; genials in two pairs, anteriormost pair trapezoidal, in contact with second and third infralabials; posterior pair roughly pentagonal, in contact with third infralabials; scale rows between genials and collar fold (along midventral line) nine, with the posteriormost scale row distinctly enlarged, smooth; posteriormost gular row enfolded posteriorly; lateral neck scales squarish or rounded, smooth.

Natural history: *Riama muchmoreorum* sp. nov. has only been recorded in forest-edge situations along dirt roads. At the type locality, individuals were found under rocks, dirt clods, as well as in crevices in dirt walls as much as 50 cm underground. The species was found living in sympatry with lizards of the genus *Pholidobolus*.

Distribution: *Riama muchmoreorum* sp. nov. is known only from the type locality, an area known as La Libertad, slightly outside the Reserva Mazar, along the Zhoray–Mazar road. The locality is in the valley of Río Mazar, on the upper watershed of the Río Paute in Cañar province. The species has only been recorded along a 1 km stretch of road at elevations of 2,664–2,765 m above sea level (Fig. 2).

Etymology: This newly discovered species of lizard is named in honor of Lile Muchmore and her family. Born into a family deeply committed to conservation and advocating for the voiceless, Lile has

been an enduring source of inspiration. Despite facing physical and cognitive challenges, she has encouraged many to embrace life fully and to cherish what is often overlooked. The Muchmore family played a pivotal role in supporting the expedition that led to the discovery of this remarkable burrowing lizard.

Conservation status: We consider *Riama muchmoreorum* sp. nov. to be Data Deficient following IUCN Red List criteria because the species belongs to a poorly studied genus of lizards and is known only from a single locality along a river valley (Río Mazar) on the eastern slopes of the Ecuadorian Andes. At this locality, most of the native cloud forest habitat has been converted to pastures. However, we consider there is insufficient data to estimate whether this new lizard species is actually restricted to an area no greater than 10 km² or if it is more widespread.

***Riama ellasabinae* sp. nov.**
https://zoobank.org/C44AB25B-9226-49C5-8C53-BFA759992EDB
Figs 14, 15, 16

Type material. Holotype: AAS-002 (Figs 14, 15a, 16), an adult male collected by Alejandro Arteaga, Angie Tovar, and Sophia Hurtado in 2023 at the Sendero Sardinayacu, Morona Santiago province, Ecuador (-2.09482, -78.12454; 1,498 m).

Paratopotype: AAS-001 (Fig. 15b), adult male. See also Suppl. material 1.

Paratypes: AMNH 38821, subadult female, Abitagua, Tungurahua province, Ecuador (-1.41667, -78.16667; 1,353 m); AMNH 38822, adult male, Abitagua, Tungurahua province, Ecuador (-1.41667, -78.16667; 1,353 m); ANSP 29116, adult male, Cordillera de Cutucú, Morona Santiago province, Ecuador (-2.64692, -78.02258; 1,975 m); FHGO 2405, adult male, Cuenca del Río Jamboé, Zamora Chinchipe, Ecuador (-4.12301, -78.94301; 1,069 m); FHGO 12406, subadult female, Las Peñas, Zamora Chinchipe, Ecuador (-3.96453, -78.48738; 1,640 m).

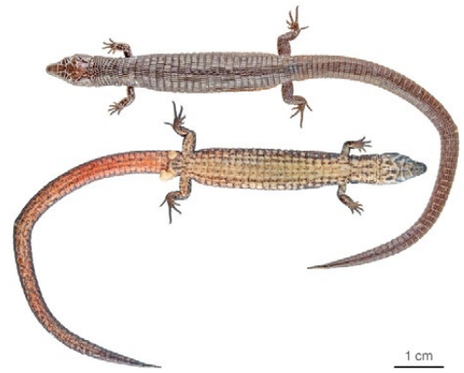

Figure 14: Holotype of *Riama ellasabinae* sp. nov. AAS 002 in dorsal and ventral view.

Proposed English name: Ella Sabin's Lightbulb Lizard.

Proposed Spanish name: Lagartija minadora de Ella Sabin.

Diagnosis: *Riama ellasabinae* sp. nov. is placed in the genus *Riama*, as diagnosed by Doan & Castoe (2005), based on phylogenetic evidence (Fig. 1). The species is diagnosed based on the following combination of characters: (1) frontonasal 0.8–1.1 × longer than frontal; (2) nasoloreal suture complete; (3) supraoculars four, usually not in contact with ciliaries; (4) 0–5 supraciliaries, usually a complete series of four; (5) supralabial-subocular fusion absent; (6) postoculars three; (7) postparietals three; (8) supratympanic temporals two or three; (9) genials two, or one in FHGO 12406, transverse sutures not perpendicular with respect to midline of body;

Figure 15: Photographs of some specimens of *Riama ellasabinae* sp. nov. in life: (a) AAS 002 adult male holotype; (b) AAS 001 adult male paratopotype.

(10) dorsals rectangular, juxtaposed, striated and keeled; (11) longitudinal dorsal scale rows in males 21, in one female 21; (12) transverse dorsal scale rows in males 35–37, in one female 35; (13) transverse ventral scale rows in males 21–23, in females 21; (14) lateral scale rows 1–2; (15) femoral pores per leg in males 8–11, in females 0–2; (16) subdigital scales on Toe I three or four; (17) limbs not overlapping when adpressed against body in adults; (18) anterior cloacal plate scales paired; (19) hemipenis capitate, with seven lateral flounces bearing large spines and seven asulcate gill-like flounces bearing small comb-like spicules; head bearing five rounded, radially arranged, fleshy protrusions; (20) dorsum reddish-brown with fine black speckling, becoming medium orange-red towards the lower flanks, with a series of dorsolateral ocelli consisting of faint black circles enclosing a bright

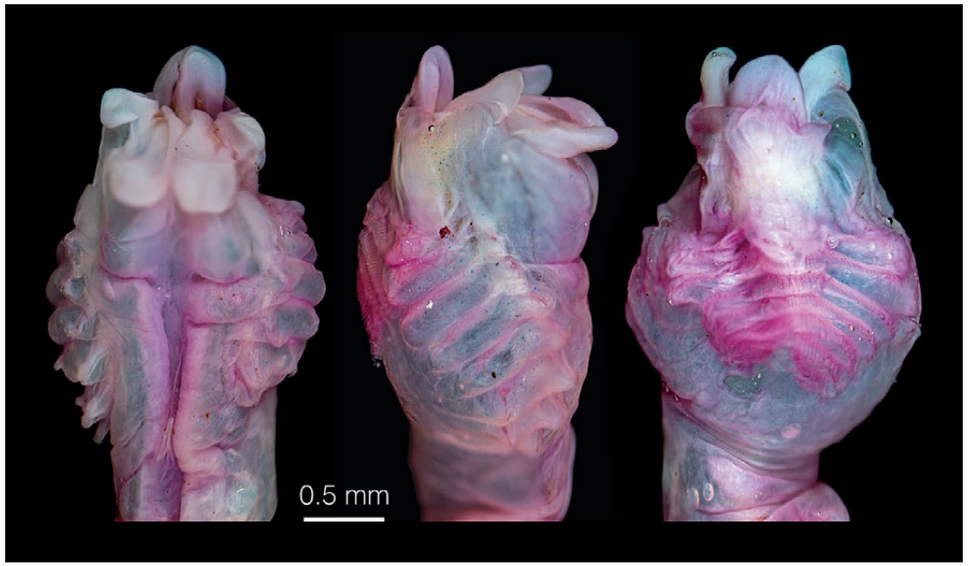

Figure 16: Hemipenial architecture of *Riama ellasabinae* sp. nov. AAS-002 holotype in sulcate, lateral, and asulcate views.

yellow spot (more prominent in males); lips dark brown with bright cream irregular spots or bars; belly and throat ochraceous (medium orange-red in breeding males) with faint dark brown speckling, forming dark brown reticulations or blotches on the throat of some individuals; underside of tail deep orange-red; (21) 49–56 mm SVL in males, 41–42 mm in females.

Comparisons: *Riama ellasabinae* sp. nov. resembles *R. anatoloros* in size, coloration, and lepidosis, but it differs from this species by having a loreal, indistinct dorsolateral stripes, a lower number of longitudinal dorsal scale rows (20–21 vs. 22–27) and transverse dorsal scale rows (35–37 vs. 38–42) in males, and by having 0–2 femoral pores in females. This species further differs from all other *Riama* for which hemipenial morphology is known, except *R. anatoloros*, by the presence of large hemipenial spines. From *R. meleagris* and *R. simotera*, the new species further differs by having striated, instead of smooth, dorsal scales. From *R. balneator*, it differs by having a lower number of transverse dorsal scale rows (35–37 vs. 42–43). From *R. cashcaensis*, it differs by having a complete nasoloreal suture as well as by lacking a ventral pattern of transverse bands. From *R. colomaromani* and *R. tarletonorum* sp. nov., it differs by being smaller in SVL and by lacking black coloration in adult males. From *R. labionis*, it differs by having a complete nasoloreal suture and by lacking supralabial-subocular fusion. From *R. orcesi*, it differs by lacking a distinct pale dorsolateral stripe above the forelimbs and hind limbs. From *R. raneyi*, it differs by having a complete nasoloreal suture and four, instead of two or three, supraoculars. From *R. stigmatoral*, it differs by having lateral ocelli. From *R. unicolor*, by having an orangish, instead of black, belly. From *R. yumborum*, it differs by having the anterior cloacal plate scales paired in males.

Hemipenial morphology: Based on the organ of AAS 002 (Fig. 16). The hemipenial body is narrow at the base and bulbous and swollen at the midpoint, ending in a slightly narrower head. The head of the hemipenis has a broad naked strip, with the distal end somewhat flattened, bearing five rounded, radially arranged, fleshy protrusions (like flower petals); a deep sulcus spermaticus, central in position, originates at the base of the organ and proceeds in a straight line towards the head. The sulcus spermaticus consists of a single channel emarginated by lobular folds with no discernible bifurcation at the head. The sulcus spermaticus is bordered on each side by a wide nude area flanked by seven rows of oblique flounces. The flounces cover the swollen globular midsection of the hemipenial body primarily on the lateral surface, with the sulcate end bearing enlarged calcified spines. The mesial asulcate surface of the hemipenial globular section has seven rows of flounces not connected to the lateral flounces and differing from the latter by being arranged like the gills of a fish and by having densely packed comb-like spicules (largely absent from the lateral flounces). These flounces spread across the asulcate surface (expansion pleat absent) and are wider distally.

Description of holotype: Male, SVL 52.7 mm, tail length 40.2 mm; head scales smooth; rostral wider than long, higher than adjacent supralabials, in contact posteriorly with nasal, frontonasal, and anterior supralabials; frontonasal trapezoidal, widest near the posterior suture, in contact laterally with nasals and loreal, posteriorly with frontal and anteriormost supraoculars; prefrontals absent; frontal longer than wide, widest anteriorly, anterior suture straight, lateral sutures slightly concave, posterior suture angular with point directed posteriorly, in contact with first and second supraoculars laterally and frontparietals posteriorly; frontoparietals pentagonal, in contact with third and fourth supraoculars laterally, parietals posterolaterally, and interparietal posteromedially; interparietal long, hexagonal, and with straight lateral sutures, in contact with parietals laterally and postparietals posteriorly; parietals hexagonal, in contact with fourth supraoculars anterolaterally, dorsalmost postoculars laterally, dorsalmost temporals posterolaterally, and postparietals posteriorly; postparietals three; supraoculars four, none in contact with ciliaries; nasoloreal suture complete; superciliaries four; palpebral disc semitransparent and divided into four large unpigmented scales; frenocular nearly trapezoidal in shape, in contact with loreal anteriorly; seven circumorbitals between posteriormost supraocular and frenocular; postoculars three; temporals smooth; supratympanic temporals 3/3; supralabials seven; infralabials five; mental wider than long, in contact with anteriormost infralabials laterally and postmental posteriorly; postmental pentagonal, posterior suture angular, with angle directed posteriorly, in contact with first and second infralabials laterally; genials in two pairs, anteriormost pair roughly pentagonal, in contact with second and third infralabials; posterior pair roughly hexagonal, in contact with third and fourth infralabials; scale rows between genials and collar fold (along midventral line) nine; medialmost scales of posteriormost scale row distinctly enlarged, smooth; posteriormost gular row enfolded posteriorly; lateral neck scales squarish or rounded, barely striated.

Natural history: *Riama ellasabinae* sp. nov. occurs in primary and secondary foothill and lower-montane evergreen for-

ests as well as in gallery forests surrounded by a matrix of pastures and plantations. The holotype and the paratopotype were found under roots and soft soil within 3–4 m of a stream in a gallery forest.

Distribution: *Riama ellasabinae* sp. nov. is known from at least 25 localities along the Amazonian foothills of the Ecuadorian Andes. The species occurs over an area of approximately 13,131 km^2 at elevations of 967–1,975 m above sea level (Fig. 2).

Etymology: Named after Ella Sabin, granddaughter of American philanthropist Andrew Sabin. The Sabin family supports conservation and field research of reptiles and has protected over 264,365 acres of critical habitat throughout the world.

Conservation status: We consider *Riama ellasabinae* sp. nov. to be Least Concern following IUCN Red List criteria (IUCN 2012) because the species is distributed over a comparatively wide region (greater than 10,000 km^2) of the Amazonian slopes of the Andes that holds large areas of continuous unspoiled forest. Based on the species distribution model presented in Fig. 2 in combination with the most recent maps of vegetation cover of the Amazon basin (MapBiomas Amazonía 2022), we estimate that approximately 81% of the species' forest habitat is still standing.

***Riama tarletonorum* sp. nov.**
https://zoobank.org/1A3C0D43-622B-4D0A-8A41-AACC72CA0EF2
Figs 17, 18, 19

Type material. Holotype: TH 787 (Figs 17, 18d, 19), adult male collected by Jose Vieira, Amanda Quezada, Frank Pichardo, and Harry Turner in 2020 at La Centella, Carchi province, Ecuador (0.81436, -78.01497; 2,806 m).

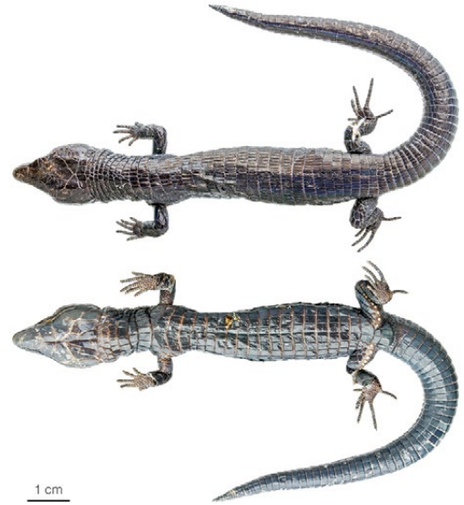

Figure 17: Holotype of *Riama tarletonorum* sp. nov. TH 787 in dorsal and ventral view.

Paratopotypes: TH 670, adult female; TH 674, juvenile female; TH 735, adult male. See also Suppl. material 1.

Paratypes: TH 659 (Fig. 18b), juvenile female; TH 660, subadult female; TH 661 (Fig. 18c), adult female; TH 666, adult male; TH 707 (Fig. 18a), adult female; TH 713, adult female; TH 715, subadult female. All seven from El Morán, Carchi province, Ecuador (0.76850, -78.05556; 2,778 m). See also Suppl. material 1.

Proposed English name: Tarletons' Lightbulb Lizard.

Proposed Spanish name: Lagartija minadora de los Tarleton.

Diagnosis: *Riama tarletonorum* sp. nov. is placed in the genus *Riama*, as diagnosed by Doan & Castoe (2005), based on phylogenetic evidence (Fig. 1). The species is diagnosed based on the following combination of characters: (1)

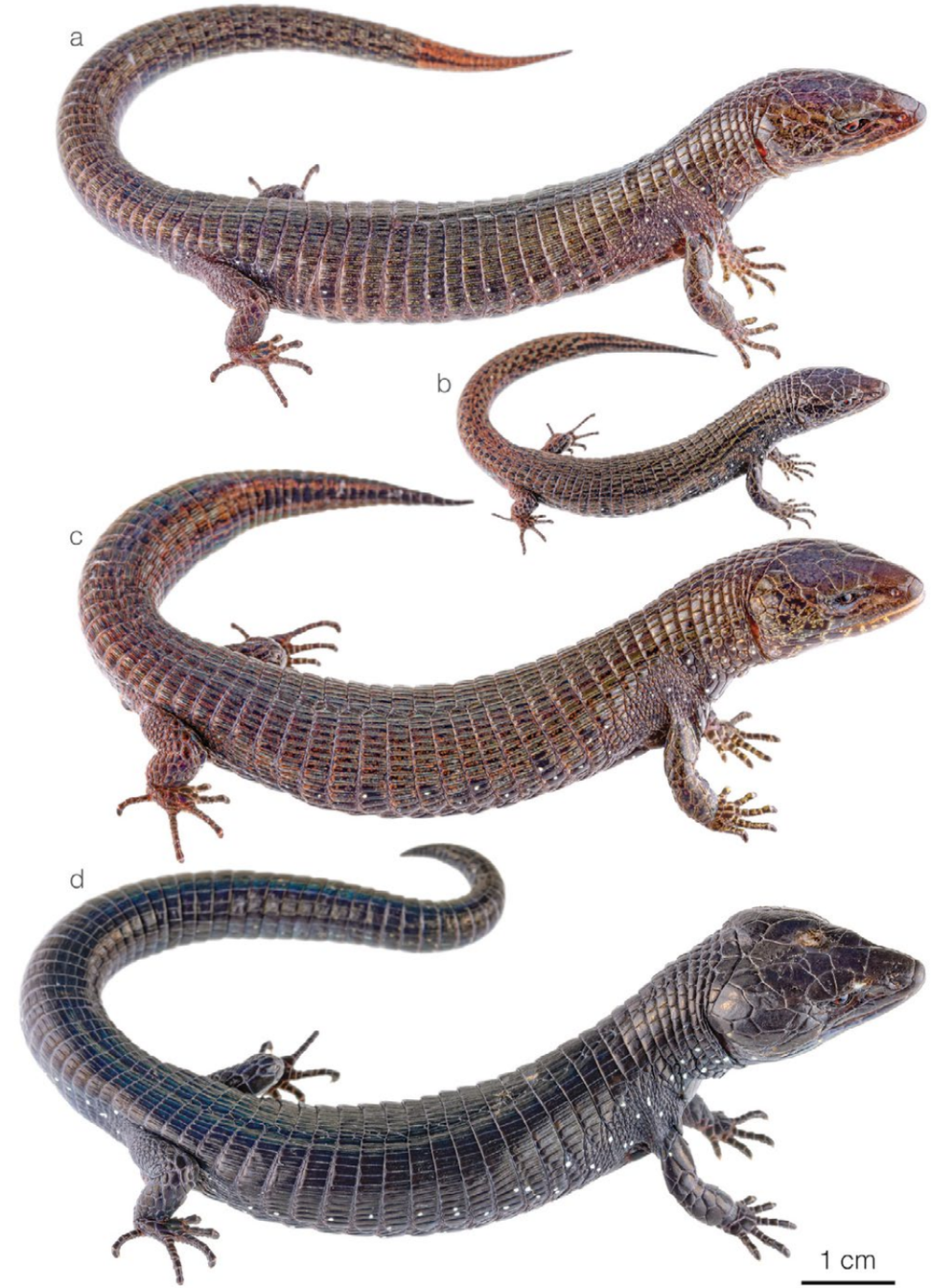

Figure 18: Photographs of some specimens of *Riama tarletonorum* sp. nov. in life: (a) TH 707 adult female from El Morán, Carchi province; (b) TH 659 juvenile female from El Morán, Carchi province; (c) TH 661 adult female from El Morán, Carchi province; (d) TH 787 holotype.

frontonasal 1.1–1.3 × longer than frontal; (2) nasoloreal suture incomplete; (3) supraoculars four, with 2nd and 4th in contact with ciliaries; (4) 0–3 supraciliaries, series incomplete; (5) supralabial-subocular fusion absent; (6) postoculars usually three; (7) postparietals two; (8) supratympanic temporals two or three; (9) genials two, posterior pair usually in narrow contact, transverse sutures not perpendicular with respect to midline of body; (10) dorsals rectangular, juxtaposed, striated/keeled; (11) longitudinal dorsal scale rows in males 21–25, in females 23–25; (12) transverse dorsal scale rows in males 35–38, in females 36–38; (13) transverse ventral scale rows in males 19–20, in females 19–21; (14) lateral scale rows 1–2; (15) femoral pores per leg in males 7–9, in females 7–8; (16) subdigital scales on Toe I four or five; (17) limbs not overlapping when adpressed against body in adults; (18) anterior cloacal plate scales paired; (19) hemipenis capitate; flounces bearing comb-like spinules, forming W-shaped chevrons continuous across the asulcate surface; asulcate flounces much narrower than sulcate flounces; asulcate expansion pleat absent; (20) dorsum of adult males black with a bluish sheen, bright white spots along the flanks, and with or without a series of ochraceous spots forming a broken dorsolateral line; dorsum of adult females blackish or dark brown with a series of faint ocelli (black circles with a white spot in the middle); ventral surfaces shiny black with the exception of the scale junctions and the throat of some individuals, which are cream; (21) 79–90 mm SVL in males, 53–75 mm in females.

Comparisons: *Riama tarletonorum* sp. nov. resembles *R. colomaromani* in size, coloration, and lepidosis, but it differs from this species by having fewer longitudinal dorsal scale rows in males (21–25 vs. 24–27) and a completely different dorsal coloration in females, consisting of a drab background with fine reddish and black speckling and flanks bearing distinct ocelli (instead of shiny black dorsal coloration with white spots along the flanks in *R. colomaromani*). From *R. anatoloros*, *R. antioquensis*, *R. balneator*, *R. orcesi*, *R. simotera*, and *R. striata*, the new species differs by having an incomplete series of superciliary scales. From *R. anatoloros* and *R. ellasabinae* sp. nov., it differs by being larger in SVL and by having black coloration in adult males. From *R. cashcaensis*, it differs by having femoral pores in females, no subcaudal transverse bands, and hemipenial flounces arranged in two chevrons (vs. two columns). From *R. columbiana* and *R. meleagris*, it differs by having striated dorsal scales and a uniform black dorsum in males. From *R. labionis*, it differs by lacking supralabial-subocular fusion and having a lower number of femoral pores in males (7–9 vs. 10–13). From *R. raneyi*, it differs by having four supraoculars (vs. two or three). From *R. stigmatoral*, it differs by having femoral pores in females and no ventrolateral spots. From *R. unicolor*, it differs by lacking subcaudal stripes as well as by having femoral pores in females. From *R. yumborum*, it differs by having 19–21 transverse rows of ventral scales (vs. 22–23) and fewer (7–9 vs. 13) femoral pores in males.

Hemipenial morphology: Based on the right organ of TH 787 (Fig. 19). The hemipenial body is nearly columnar, tapered toward the base, ending in two symmetric small and partially everted lobes outlined by folds; a shallow sulcus spermaticus, central in position, originates at the base of the organ and proceeds in a straight line towards the lobes. The sulcus spermaticus consists of a single channel

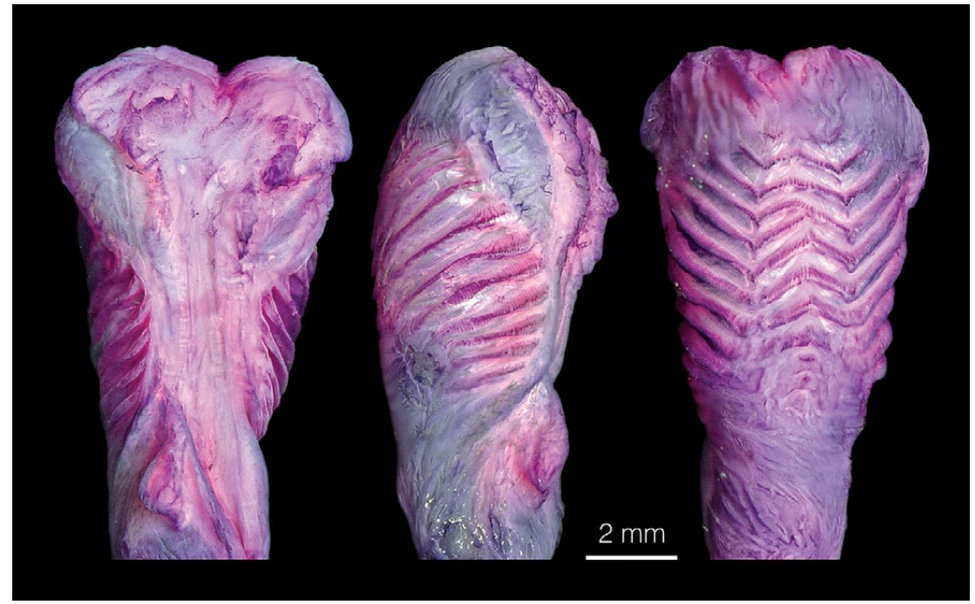

Figure 19: Hemipenial architecture of *Riama tarletonorum* sp. nov. TH 787 holotype in sulcate, lateral, and asulcate views.

emarginated by lobular folds and ending in a barely discernible bifurcation at the head. The sulcus spermaticus is bordered on each side by a narrow nude area flanked by eight rows of oblique flounces. The flounces cover the distal portion of the hemipenial body on both lateral and asulcate views, where they are more numerous (ten or eleven) and bear comb-like spicules. The flounces are arranged in W-shaped rows continuous across the asulcate surface (asulcate expansion pleat absent), extending to the borders of each nude area contiguous to the sulcus spermaticus. The distal flounces on the sulcate face bear no discernible spicules.

Description of holotype: Male, SVL 89.5 mm, tail (incomplete) length 87 mm; head scales smooth to slightly rugose; rostral wider than long, higher than adjacent supralabials, in contact posteriorly with nasal, frontonasal, and anteriormost supralabials; frontonasal rounded trapezoidal in shape, widest near the posterior suture, 1.2 × longer than frontal, in contact laterally with nasals and posteriorly with frontal and anteriormost supraoculars; prefrontals absent; frontal longer than wide, widest anteriorly, anterior suture slightly convex, lateral sutures slightly concave, in contact with first and second supraoculars laterally and frontoparietals posteriorly; frontoparietals pentagonal, with the sutures of the right one obscured by scarred tissue, in contact with third supraoculars laterally, parietals posterolaterally, and interparietal posteromedially; interparietal long, hexagonal, and with slightly concave lateral sutures, in contact with parietals laterally and postparietals posteriorly; parietals hexagonal, in contact with fourth supraoculars anterolaterally, dorsalmost postoculars laterally, dor-

salmost temporals posterolaterally, and postparietals posteriorly; postparietals two, longest laterally, in contact medially; supraoculars four, with second, third, and fourth in contact with ciliaries; nasoloreal suture incomplete; superciliary single, located anteriorly and situated between nasal, frontal, frontonasal, first and second supraoculars, and anteriormost ciliaries, barely extending onto the dorsal surface of the head; palpebral disc semitransparent and divided into four large unpigmented scales; frenocular nearly trapezoidal in shape, in contact with nasal anteriorly; six circumorbitals between posteriormost supraocular and frenocular; postoculars three; temporals smooth; supratympanic temporals 2/2; supralabials seven; infralabials six; mental wider than long, in contact with anteriormost infralabials laterally and postmental posteriorly; postmental roughly pentagonal, posterior suture angular, with angle directed posteriorly, in contact with first and second infralabials laterally; genials in two pairs, anteriormost pair roughly pentagonal, in contact with second and third infralabials; posterior pair hexagonal, in contact with third and fourth infralabials; scale rows between genials and collar fold (along midventral line) eight; medialmost scales of posteriormost scale row enlarged, smooth; posteriormost gular row enfolded posteriorly; lateral neck scales squarish, rugose.

Natural history: *Riama tarletonorum* sp. nov. occurs in high Andean ecosystems consisting of a matrix of remnants of high evergreen montane forests and pastures. Individuals were found under rocks, buried under soft dark soil, or in dirt walls among roots and rotten logs.

Distribution: *Riama tarletonorum* sp. nov. is known only from three localities (listed under Suppl. material 3) on the upper watershed of the Río La Plata in Carchi province. The species occurs over an area of approximately 20 km² and has been recorded at elevations of 2,728–2,825 m above sea level (Fig. 2).

Etymology: This new species of lizard is named after the Tarleton family of Austin, Texas (Stephen, Marissa, Owen, and Charlotte), all passionate about travel, nature, and conservation. The Tarletons helped fund the expedition that resulted in the discovery of this new species of burrowing lizard.

Conservation status: We consider *Riama tarletonorum* sp. nov. to be Data Deficient following IUCN Red List criteria because the species belongs to a poorly studied genus of lizards and is known only from three localities along a single river valley (Río La Plata) on the western slopes of the Ecuadorian Andes. At one of the localities, El Morán, most of the native cloud forest habitat has been converted to pastures. However, we consider there is insufficient data to estimate whether this new lizard species is restricted to an area no greater than 20 km² or if it ranges into Colombia.

DISCUSSION

This work represents the third major effort to clarify the species limits of Ecuadorian lightbulb lizards (genus *Riama*) using an integration-by-congruence approach. Our results provide evidence for 18 species of *Riama* in Ecuador, six of which are described here as new.

We confirm Kizirian's (1996) suspicion that populations of *Riama colomaromani* from Carchi province represent a distinct species. However, contrary to that author's suggestions, we found that lateral scale rows, frontonasal length, and the contact between posterior genials are not reliable diagnostic characters for distinguishing between *R. colomaromani* and the new species. Instead, female coloration proves to be the most effective diagnostic trait.

Our analysis reveals that *Riama unicolor sensu lato* comprises three species, which are easily distinguished by hemipenial morphology, the coloration of the tail underside, and the number of supraoculars, transverse ventral scale rows, and transverse dorsal scale rows. We highlight that the holotype of *R. unicolor* has an uncertain type locality and, as noted by Kizirian (1996), possesses four supraoculars—a trait found in only 7.6% of the *R. unicolor sensu lato* specimens he examined. It remains unclear which population the holotype belongs to, as all *R. unicolor sensu stricto* specimens examined in this study possess only two or three supraoculars.

Similarly, we found that *Riama stigmatoral sensu lato* consists of three species diagnosable by ventral coloration, the condition of the nasoloreal suture, the number of longitudinal ventral scale rows, and the number of femoral pores in males. These three species occupy distinct Andean watersheds and versants: *R. stigmatoral sensu stricto* is restricted to the Río Negro watershed on the Amazonian slopes of Morona Santiago province, while *R. muchmoreorum* sp. nov. and *R. jenningsi* sp. nov. occur in inter-Andean valleys of the upper Río Paute watershed. Notably, there have been no recent collections of *R. stigmatoral sensu stricto* from its type locality (the old trail between Sevilla de Oro and Méndez), leaving these populations unsampled for molecular data.

Reanalyzing the molecular data from Sánchez-Pacheco et al. (2018) revealed deep genetic differentiation between the northern and southern populations of *Riama anatoloros* sensu lato. Although we did not expand the molecular sampling, we utilized morphological characters—including the presence of a loreal, the condition of dorsolateral stripes, scale row counts in males, and femoral pore counts in females—to distinguish *R. anatoloros sensu stricto* from *R. ellasabinae* sp. nov. Comprehensive molecular sampling across their respective ranges is needed to refine their distributions and may reveal additional undescribed taxa.

While this study advances the taxonomy of Ecuadorian *Riama*, several gaps remain. First, obtaining molecular data from the *R. unicolor* holotype is essential to restrict its type locality and evaluate the diagnostic value of supraocular counts. Second, fresh material from the type locality of *R. stigmatoral* is required to confirm if populations from the Tinajillas–Río Gualaceño area belong to that species. Finally, molecular sampling of northern populations of *R. ellasabinae* sp. nov. is imperative to determine its distribution, which potentially extends into Peru.

Future systematic revisions of *Riama* should prioritize expanded geographic sampling and multi-locus data. Such studies would benefit significantly from sampling historical type material and populations from southern Colombia. We hope this work provides a foundation for future biogeographic studies of this enigmatic group.

ACKNOWLEDGMENTS

This article was greatly improved by comments of two anonymous reviewers. We are indebted to David Kizirian for his help and guidance during AA's time at the

AMNH as well as for suggesting that some populations of *Riama* in northern Ecuador were probably new species. For granting access to museum specimens under their care, we are grateful to Christopher Raxworthy (AMNH), Ned Gilmore (ANSP), and María Elena Barragán (FHGO). Thanks to Juan M Guayasamin (Laboratorio de Biología Evolutiva, USFQ) for providing lab infrastructure, reagents, and personnel time during earlier versions of the project that lead to this publication. For granting access to the protected forests under their care, we are grateful to Martin Schaefer and David Agro (Fundación Jocotoco), Giovanni Onore (Fundación Otonga), Stuart White (Fundación Cordillera Tropical), Patricio Estrella (Área Ecológica de Conservación Municipal Tinajillas – Río Gualaceño), and Holger Santos (Santa Lucía Cloud Forest Reserve). Special thanks to Alex Pyron, Amadeus Plewnia, Ana Tufiño, Carlos Nivelo, Eric Osterman, Frank Pichardo, Gabriela Morales, Gabriella Marcano, Harry Turner, Jorge Luis Romero, María José Quiroz, Matilde Navarro, and Sophia Hurtado for their assistance and companionship in the field. Diana Encalada examined fluid-preserved specimens and created photographs of the material referenced here. Fieldwork was made possible with the support of Walter Jennings (Fundación Jocotoco), Casey Klebba and Carly Jones (Minifund), Khamai Foundation, Tropical Herping, Savia Fund, Liberty University, Francis Marion University, Joseph Higgins, Alain Kormann, Suzana Lightman, James Muchmore, John Sullivan, Daniel Zamora-Valdés, Christian Cave, Brian Monk, Roy and Laurie Averill-Murray, Lois Yuen, and Phillip Lietz. Sequencing was made possible with support of the Inédita Program from the Ecuadorian Science Agency SENESCYT (INEDITA PIC-20-INE-USFQ-001).

REFERENCES

Aguirre-Peñafiel V, Torres-Carvajal O, Nunes PM, Peck MR, Maddock ST (2014) A new species of *Riama* Gray, 1858 (Squamata: Gymnophthalmidae) from the Tropical Andes. Zootaxa 3866: 246–260.

Arévalo E, Davis SK, Sites JW (1994) Mitochondrial DNA-sequence divergence and phylogenetic relationships among eight chromosome races of the *Sceloporus grammicus* complex (Phrynosomatidae) in Central Mexico. Systematic Biology 43: 387–418.

Arteaga A, Bustamante L, Vieira J (2024) Reptiles of Ecuador: Life in the middle of the world. Khamai Foundation & Tropical Herping, Quito, 1075 pp.

Beaupre SJ, Jacobson ER, Lillywhite HB, Zamudio K (2004) Guidelines for use of live amphibians and reptiles in field and laboratory research. American Society of Ichthyologists and Herpetologists, Lawrence, 43 pp.

Burbrink FT, Crother BI, Murray CM, Smith BT, Ruane S, Myers EA, Pyron RA (2022) Empirical and philosophical problems with the subspecies rank. Ecology and Evolution, 12: e9069.

Caliński T, Harabasz J (1974) A dendrite method for cluster analysis. Communications in Statistics 3: 1–27.

Carbayo F, Marques AC (2011) The costs of describing the entire animal kingdom. Trends in Ecology & Evolution 26: 154–155.

Carstens BC, Pelletier TA, Reid NM, Satler JD (2013) How to fail at species delimitation. Molecular Ecology 22: 4369–4383.

Cisneros-Heredia DF (2005) *Saphenophis boursieri*. Habitat, reproduction and diet. Herpetological Review 36: 71.

de Queiroz K (2007) Species concepts and species delimitation. Systematic Biology 56: 879–886.

Doan TM, Castoe TA (2005) Phylogenetic taxonomy of the Cercosaurini (Squamata: Gymnophthalmidae), with new genera for species of *Neusticurus* and *Proctoporus*. Zoological Journal of the Linnean Society 143: 405–416.

Dowling HG, Savage JM (1960) A guide to the snake hemipenis: a survey of basic structure and systematic characteristics. Zoologica 45: 17–28.

Drummond AJ, Ashton B, Buxton S, Cheung M, Cooper A, Heled J, Kearse M, Moir R, Stones-Havas S, Sturrock S, Thierer T, Wilson A (2021) Geneious version 2021.1.

Elith J, Leathwick JR (2009) Species distribution models: ecological explanation and prediction across space and time. Annual Review of Ecology, Evolution, and Systematics 40: 677–697.

Elith J, Phillips SJ, Hastie T, Dudík M, Chee YE, Yates CJ (2011) A statistical explanation of MaxEnt for ecologists. Diversity and Distributions 17: 43–57.

Felsenstein J (2004) Inferring phylogenies. Sinauer Associates, Sunderland, 664 pp.

Gould J, Valdez JW (2022) The Gollum Effect: the issue of research opportunity guarding in Academia. Frontiers in Ecology and Evolution. 10: 889236.

Gray JE (1858) Description of *Riama*, a new genus of lizards, forming a distinct family. Proceedings of the Zoological Society of London 1: 441–443.

Greenacre M (2007) Correspondence Analysis in Practice. Chapman and Hall/CRC, New York, 296 pp.

Hartigan JA, Wong MA (1979) Algorithm AS 136: A k-means clustering algorithm. Journal of the Royal Statistical Society: Series C (Applied Statistics) 28: 100–108.

Hijmans RJ, Cameron SE, Parra JL, Jones PG, Jarvis A (2005) Very high resolution interpolated climate surfaces for global land areas. International Journal of Climatology 25: 1965–1978.

IUCN (2012) IUCN Red List categories and criteria: Version 3.1. Second edition. IUCN Species Survival Commission, Gland and Cambridge, 32 pp.

Jost L, Yanez-Muñoz MH, Brito J, Reyes-Puig C, Reyes-Puig JP, Guayasamin JM, Ron SR, Quintana C, Iturralde G, Baquero L, Monteros M, Freire-Fierro A, Fernández D, Mendieta-Leiva G, Morales JF, Karremans AP, Vázquez-García JA, Salazar GA, Hágsater E, Solano R, Fernández-Concha GC, Arana M (2023) Eponyms are important tools for biologists in the Global South. Nature Ecology and Evolution 7: 1164–1165.

Kaiser HF (1958) The varimax criterion for analytic rotation in factor analysis. Psychometrika 23: 187–200.

Kassambara A, Mundt F (2020) Factoextra: Extract and visualize the results of multivariate data analyses. R package version 1.0.7.

Katoh K, Standley DM (2013) MAFFT multiple sequence alignment software version 7: improvements in performance and usability. Molecular Biology and Evolution 30: 772–780.

Kizirian DA (1996) A review of Ecuadorian *Proctoporus* (Squamata: Gymnophthalmidae) with descriptions of nine new species. Herpetological Monographs 10: 85–155.

Kizirian DA, Coloma LA (1991) A new species of *Proctoporus* (Squamata: Gymnophthalmidae) from Ecuador. Herpetologica 47: 420–429.

Kocher TD, Thomas WK, Meyer A, Edwards SV, Pääbo S, Villablanca FX, Wilson AC (1989) Dynamics of mitochondrial DNA evolution in animals: amplification and sequencing with conserved primers. Proceedings of the National Academy of Sciences of the United States of America 86: 6196–6200.

Lanfear R, Frandsen PB, Wright AM, Senfeld T, Calcott B (2016) PartitionFinder 2: new methods for selecting partitioned models of evolution for molecular and morphological phylogenetic analyses. Molecular Biology and Evolution 34: 772–773.

Lê S, Josse J, Husson F (2008) FactoMineR: An R package for multivariate analysis. Journal of Statistical Software 25: 1–18.

Lleonart J, Salat J, Torres GJ (2000) Removing allometric effects of body size in morphological analysis. Journal of Theoretical Biology 205: 85–93.

MAE (2012) Línea base de deforestación del Ecuador continental. Ministerio del Ambiente del Ecuador, Quito, 30 pp.

Maechler M, Rousseeuw P, Struyf A, Hubert M, Hornik K (2023). Cluster: Cluster Analysis Basics and Extensions. R package v.2.1.4.

MapBiomas Amazonía (2022) Mapeo anual de cobertura y uso del suelo de la Amazonía.

O'Shaughnessy AWE (1879) Descriptions of new species of lizards in the collection of the British Museum. Annals and Magazine of Natural History 5: 295–303.

Padial JM, Miralles A, de la Riva I, Vences M (2010) The integrative future of taxonomy. Frontiers in Zoology 7: 16.
Palumbi SR, Martin A, Romano S, McMillan WO, Stice L, Grabowski G (1991) The simple fool's guide to PCR, version 2.0. University of Hawaii, Honolulu, 94 pp.
Peñafiel N, Flores DM, Rivero De Aguilar J, Guayasamin JM, Bonaccorso E (2020) A cost-effective protocol for total DNA isolation from animal tissue. Neotropical Biodiversity 5: 69–74.
Pesantes OS (1994) A method for preparing hemipenis of preserved snakes. Journal of Herpetology 28: 93–95.
Peterson AT, Soberón JR, Pearson RG, Anderson RP, Martínez-Meyer E, Nakamura M, Bastos Araújo M (2011) Ecological niches and geographic distributions. Princeton University Press, Princeton, 328 pp.
Phillips SJ, Anderson RP, Schapire RE (2006) Maximum entropy modeling of species geographic distributions. Ecological Modelling 190: 231–259.
R Core Team (2023) R: A language and environment for statistical computing. R Foundation for Statistical Computing, Vienna.
Rambaut A, Suchard M, Drummond AJ (2022) Tracer version 1.7.1.
Renner IW, Warton DI (2013) Equivalence of MAXENT and poisson point process models for species distribution modeling in ecology. Biometrics 69: 274–281.
Ronquist F, Huelsenbeck JP (2013) MrBayes 3: Bayesian phylogenetic inference under mixed models. Bioinformatics 19: 1572–1574.
Rousseeuw PJ (1987) Silhouettes: A graphical aid to the interpretation and validation of cluster analysis. Journal of Computational and Applied Mathematics 20: 53–65.
Royle JA, Chandler RB, Yackulic C, Nichols JD (2012) Likelihood analysis of species occurrence probability from presence-only data for modelling species distributions. Methods in Ecology and Evolution 3: 545–554.
Saint KM, Austin CC, Donnellan SC, Hutchinson MN (1998) C-mos, a nuclear marker useful for squamate phylogenetic analysis. Molecular Phylogenetics and Evolution 10: 259–263.
Sánchez-Pacheco SJ, Torres-Carvajal O, Aguirre-Peñafiel V, Sales-Nunes PM, Verrastro L, Rivas GA, Rodrigues MT, Grant T, Murphy RW (2018) Phylogeny of *Riama* (Squamata: Gymnophthalmidae), impact of phenotypic evidence on molecular datasets, and the origin of the Sierra Nevada de Santa Marta endemic fauna. Cladistics 34: 260–291.
Soberón J, Peterson TA (2005) Interpretation of models of fundamental ecological niches and species' distributional areas. Biodiversity Informatics 2: 1–10.
Thorndike RL (1953) Who belongs in the family? Psychometrika 18: 267–276.
Thorpe RS (1975) Quantitative handling of characters useful in snake systematics with particular reference to *Trimeresurus* and the results obtained for *T. puniceus*. Biological Journal of the Linnean Society 7: 27–43.
Torres-Carvajal O, Lobos SE, Venegas PJ, Chávez G, Aguirre-Peñafiel V, Zurita D, Echevarría LY (2016) Phylogeny and biogeography of the most diverse clade of South American gymnophthalmid lizards (Squamata, Cercosaurinae). Molecular Phylogenetics and Evolution 99: 63–75.
Tschudi JJ (1845) Reptilium conspectum quae in republica Peruana reperiuntur er pleraque observata vel collecta sunt in itenere. Archiv für Naturgeschichte 11: 150–170.
Valdez JW, Sharma S, Gould J (2025) Systemic territoriality in academia: The Gollum effect's impact on scientific research and careers. One Earth 8, 101314.
Weihs C, Ligges U, Luebke K, Raabe N (2005) klaR: Analyzing German business cycles. In: Bair D, Decker R, Schmidt-Thieme L (Eds) Data Analysis and Decision Support, Springer, Berlin, 335–343 pp.
Wickham H (2016) ggplot2: Elegant graphics for data analysis. Springer-Verlag, New York, 213 pp.
Wüster W (2025) Shedding the mitochondrial blinkers: A long-overduechallenge for species delimitation in herpetology. Vertebrate Zoology 75: 259–275.
Zaher H (1999) Hemipenial morphology of the South American xenodontine snakes, with a proposal for a monophyletic Xenodontinae and a reappraisal of colubroid hemipenes. Bulletin of the American Museum of Natural History 240: 1–168.

APPENDIX 1

Table A1: List of PCR and sequencing primers and their respective PCR conditions (denaturation, annealing, extension, and number of cycles) used in this study. PCR protocols included an initial 3-min step at 94 °C and a final extension of 10 min at 72 °C.

Locus	Primer	Sequence (5'-3')	Reference	PCR profile
12S	12S1L	CAAACTGGGATTAGATACCCCACTAT	Kocher et al. 1989	92 °C (30 sec), 57 °C (30 sec), 72 °C (1:50 min) [x33]
	12S2H	AGGGTGACGGGCGGTGTGT		
16S	16Sar-L	CGCCTGTTTATCAAAAACAT	Palumbi et al. 1991	94 °C (45 sec), 53 °C (45 sec), 72 °C (1 min) [x30]
	16Sbr-H-R	CCGGTCTGAACTCAGATCACGT		
ND4	ND4	CACCTATGACTACCAAAAGCTCATGTAGAAGC	Arévalo et al. 1994	94 °C (25 sec), 56 or 60 °C (1 min), 72 °C (2 min) [x25–30]
	Leu	CATTACTTTTACTTGGATTTGCACCA		
CMOS	G73	GCGGTAAAGCAGGTGAAGAAA	Saint et al. 1998	95 °C (30 sec), 52 °C (1 min), 72 °C (1 min) [x40]
	G74	TGAGCATCCAAAGTCTCCAATC		

SUPPLEMENTARY MATERIAL 1

Morphological and locality data
Author: Alejandro Arteaga
Data type: xlsx
Explanation note: Morphological and locality data for specimens of *Riama* examined, either directly or indirectly through digital photographs.
Codes: SVL=snout-vent length, CL=Caudal length, M=Male, F=Female.

DOI: 10.6084/m9.figshare.32400195

SUPPLEMENTARY MATERIAL 2

GenBank accession numbers
Author: Alejandro Arteaga
Data type: xlsx
Explanation note: GenBank accession numbers for loci and terminals of taxa and outgroups sampled in this study. Novel sequence data produced in this study are marked with an asterisk (*).

DOI: 10.6084/m9.figshare.32400288

SUPPLEMENTARY MATERIAL 3

Locality data
Author: Alejandro Arteaga
Data type: xlsx
Explanation note: Coordinates represent actual GPS readings taken at the locality of collection or georeferencing attempts from gazetteers under standard guidelines, although some variation from the exact collecting locality will be present. Similarly, elevations are taken from Google Earth and may not exactly match the elevations as originally reported.

DOI: 10.6084/m9.figshare.32400306

SUPPLEMENTARY MATERIAL 4

Morphometric analyses
Author: Angie Tovar-Ortiz
Data type: docx
Explanation note: Based on selected variables in Supplementary material 1.

DOI: 10.6084/m9.figshare.32400318